available at www.sciencedirect.com

ScienceDirect

journal homepage: www.elsevier.com/locate/jhydrol

Review

A comparative review of upscaling methods for solute transport in heterogeneous porous media

Christophe C. Frippiat *,1, Alain E. Holeyman

Department of Civil and Environmental Engineering, Université catholique de Louvain, Place du Levant 1, B-1348 Louvain-la-Neuve, Belgium

Summary   The classical Fickian model for solute transport in porous media cannot correctly predict the spreading (the dispersion) of contaminant plumes in a heterogeneous subsurface unless its structure is completely characterized. Although the required precision is outside the reach of current field characterization methods, the advection—dispersion model remains the most widely used model among practitioners. Two approaches can be adopted to solve the effect of physical heterogeneity on transport. First, based on a given characterization of the spatial structure of the subsurface, upscaling methods allow the computation of apparent scale-dependent parameters (especially longitudinal dispersivity) to be used in the classical Fickian model. In the second approach, upscaled (non-Fickian) transport equations with scale-independent parameters are used. In this paper, efforts are made to classify and review upscaling methods for Fickian transport parameters and non-Fickian upscaled transport equations for solute transport, with an emphasis on their mathematical properties and their (one-dimensional) analytical formulations. In particular, their capacity to model scale effects in apparent longitudinal dispersion is investigated. Upscaling methods and upscaled models are illustrated in the case of two three-dimensional synthetic aquifers, with lognormal hydraulic conductivity distributions characterized by variance values of 2 and 8.
© 2008 Elsevier B.V. All rights reserved.

---

* Corresponding author. Tel.: +1 303 384 2237.
  E-mail address: cfrippia@mines.edu (C.C. Frippiat).
1 Present address: Center for Experimental Study of Subsurface Environmental Processes (CESEP), Colorado School of Mines, 1500 Illinois Street, Golden, CO 80401, USA.

Contents

Introduction

The classical model for solute transport in the subsurface is the advection–dispersion equation (ADE). It embodies advection, molecular diffusion and mechanical dispersion as mass transfer processes

$$\frac{\partial C}{\partial t} = -\sum_i \frac{\partial}{\partial x_i}\left(q_i^A + q_i^d + q_i^D\right) \tag{1}$$

where C is the solute concentration, t is the time and x_i is the spatial coordinate in direction i. $q_i^A = v_i C$ is the advective mass flux in direction i, v_i being the velocity. The diffusive mass flux is computed using Fick's first law $q_i^d = -D^d \partial C / \partial x_i$, where D^d is an effective diffusion coefficient. Local dispersion is a physical mechanism of spreading caused by microscale variability in the velocity field. It is classically modeled using a Fickian law $q_i^D = -\sum_j D_{ij}\partial C/\partial x_j$. Diffusion and dispersion are usually combined in a single tensor $D_{ij}^H = D^d + D_{ij}$ called hydrodynamical dispersion. Substitution of mass fluxes in (1) yields

$$\frac{\partial C}{\partial t} = -\sum_i v_i \frac{\partial C}{\partial x_i} + \sum_i \sum_j \frac{\partial}{\partial x_i}\left(D_{ij}^H \frac{\partial C}{\partial x_j}\right) \tag{2}$$

In a one-dimensional framework, it simplifies to

$$\frac{\partial C}{\partial t} = -v \frac{\partial C}{\partial x} + D_L \frac{\partial^2 C}{\partial x^2} \tag{3}$$

where $x = x_1$, $v = v_1$ and $D_L = D_{11}^H$ [m^2/s] is the longitudinal hydrodynamical dispersion coefficient.

The coefficient of mechanical dispersion is found to depend on the advective velocity. The exact relationship between these two parameters can however only be obtained from theoretical considerations for simple or hypothetical pore systems (Bear, 1972; de Josselin de Jong, 1958). Except in the case of very simple conceptual models, the coefficient of mechanical dispersion is generally linearly related to velocity (Bear, 1972)

$$D_{ij} = \sum_k \sum_l \alpha_{ijkl} \frac{v_k v_l}{\|v\|} \tag{4}$$

where α_{ijkl} [m] is a fourth-order tensor called dispersivity, assumed to depend only on soil properties, and $\|v\|$ is the norm of the velocity vector. In the case of an isotropic homogeneous medium, owing to symmetry properties, the dispersivity tensor can be fully described by two parameters α_L and α_T, respectively called longitudinal and transverse dispersivity (Bear, 1972), both expressed in length units. In a uniform flow field, if the principal directions of the dispersion tensor are aligned with the principal directions of the velocity field, we have

$$D_L = \alpha_L v + D^d \tag{5}$$
$$D_T = \alpha_T v + D^d \tag{6}$$

where D_L is already used in (3) and $D_T = D_{22}^H = D_{33}^H$ quantifies mechanical dispersion in a direction transverse to flow.

An extensive experimental validation of (4) was performed. Reference books usually provide plots of the longitudinal dispersion versus velocity and show that in the laboratory (5) and (6) are valid under typical groundwater flow conditions (Bear, 1972; Domenico and Schwartz, 1998; Fetter, 1999; Greenkorn, 1983). Other studies were also conducted at larger scale. For example, Klotz et al. (1980) investigated in the laboratory and in the field a more general relationship $D_L = \alpha_L v^B + D^d$ and found that parameter B should be close to one. They also showed the dependency of longitudinal dispersivity to soil sedimentological properties.

Although supported by several theoretical models and verified under well-controlled laboratory conditions and for transport in homogeneous aquifers (e.g. Taylor and Howard, 1987), the Fickian model of dispersion has shown its limits when predicting solute transport under certain other conditions. Dispersion is basically an advective process, as it is caused by variations in fluid velocity. However, such variations do not only take place at the pore scale, but also occur at larger scales, ranging from macroscopic to

megascopic (Domenico and Schwartz, 1998; Fetter, 1999; Vogel and Roth, 2003). At the field scale, commonly encountered geological structures influence contaminant transport drastically, leading to velocity variations over several orders of magnitude. This includes the effects of stratification and the presence of lenses with higher or lower permeability. Preferential pathways, such as fractures, can also lead to anomalous transport (Hauns et al., 2001). At the megascopic scale, differences between geologic formations also cause non-ideality in solute transport. As the flow path increases in length, a solute plume can encounter greater and greater variations in the aquifer, causing the variability of the velocity field to increase. Because dispersivity is related to the variability of velocity, neglecting or ignoring the true velocity distribution (i.e. by replacing the heterogeneous medium by an equivalent homogeneous one) must be compensated for by a corresponding higher apparent dispersivity (or macrodispersivity), leading to what is commonly called the scale effect of dispersion (Fetter, 1999; Fried, 1975).

This scale effect first arose from the comparison of laboratory and field values of dispersivity. Whereas typical values of dispersivity from column experiments range between 0.01 and 0.1 m, values of macroscopic dispersivity are in general three to four orders of magnitude larger (Gelhar et al., 1992; Lallemand-Barrès and Peaudecerf, 1978). It has also been widely observed that field-scale dispersion coefficients increase with distance and with time (Sauty, 1978, 1980). This scale effect was also demonstrated using controlled laboratory experiments, e.g. by Silliman and Simpson (1987).

The main challenge in addressing the scale effect of dispersion lies in finding a proper characterization of the processes occurring at scales between the laboratory scale and the megascopic scale. While microscopic processes (at the centimeter scale and below) are usually well understood, and while classical field methods generally allow a proper characterization of large geologic units (at the kilometer scale), hydraulic conductivity will vary in complicated ways at an intermediate scale (from the decimeter to the kilometer scale). Three main research directions have been investigated for the past 20 years, to improve the characterization of the spatial structure of the subsurface and the identification of hydraulic properties variations at such intermediate scale. First, field and laboratory characterization methods have received a growing attention. The advancing edge of geophysics provides new methods, such as time-domain reflectometry (Javaux and Vanclooster, 2003), ground penetrating radar (Lambot et al., 2004) or electrical resistivity tomography (Kemna et al., 2002; Slater et al., 2000), that are currently being applied to the characterization of subsurface transport problems (see also Chen et al. (2001) and Hubbard et al. (2001)).

While geophysical methods contribute largely to the improvement of soil characterization at intermediate scales (Hubbard and Rubin, 2000), their results are usually affected by larger uncertainties. As hydraulic properties of subsurface materials cannot be fully characterized in a deterministic way, stochastic methods must be invoked. Stochastic analysis provides upscaling methods that enable the variability in flow and transport to be related to the variability and the spatial structure associated to hydraulic properties of the heterogeneous medium under consideration. Most of these methods are based on a geostatistical description of the heterogeneity, either assuming finite correlation lengths (Dagan, 1984; Gelhar and Axness, 1983) or not (Zhan and Wheatcraft, 1996). Methods adapted to discrete permeability distributions were also developed (Eames and Bush, 1999).

Since classical stochastic approaches allow the computation of apparent flow and transport parameters, the advection—dispersion equation must be valid at the scale of interest and concentration distributions needs to be Gaussian. Studies have shown that after a sufficiently long travel time, according to the Central Limit Theorem, solute plumes indeed tend to have a Gaussian shape (Fiori et al., 2003a; Jankovic et al., 2006). However, for intermediate times, this observation cannot usually be made. Therefore, a third main research area focuses on the upscaling of the transport equation itself. Higher-order and fractional-order partial differential equations were either developed or brought to the field of hydrogeology (Benson et al., 2000a; Berkowitz and Scher, 1995; Cushman, 1991; Cushman and Ginn, 1993; Neuman and Orr, 1993; Scheidegger, 1960).

In this paper, a classification of existing modeling approaches is proposed and theoretical models are reviewed with an emphasis on their mathematical formulations and their capacities to model the scale effect in longitudinal dispersion. We make the difference between upscaling methods for Fickian transport parameters (section ''Upscaling methods for longitudinal dispersivity'') and non-Fickian upscaled transport equations (section ''Upscaled transport equations''), and we evaluate their capabilities to predict inert solute transport in saturated heterogeneous media. A similar review was already proposed by Zhou and Selim (2003), without mentioning inclusion models, telegraph equations, or Continuous Time Random Walks (CTRW). The review by Cushman et al. (2002) goes along the same lines of this paper. They however provide a more general mathematical formalism for the methods and provide more details on homogenization and mixtures theories, which are only mentioned in this paper. The methods and models are illustrated and compared based on two particular three-dimensional reference examples. From this point of view, this work also goes along the lines of Trefry et al. (2003), by providing an extended theoretical background for the various models and by investigating three-dimensional situations rather than two-dimensional ones.

Reference examples

A conceptual example is used as a basis for the comparison of upscaling methods and upscaled equations. This example will not be used to provide a rigorous and extensive comparison of the models and methods. It will rather be used to illustrate their respective performances in a simple but realistic situation. The reference example is therefore designed to be simple enough for allowing an easy application of all methods and models, while still incorporating a wide range of potential physical processes.

Flow and transport are numerically simulated in a 512 m long, 128 m wide and 128 m thick, three-dimensional

confined aquifer model. The grid size ΔL is constant and equal to 1 m, yielding a total of 8,388,608 cubic cells. Left ($X = 0$ m) and right ($X = 512$ m) boundaries are fixed-head boundaries in order to impose a mean gradient $J = 1\%$ in the longitudinal direction, whereas upper ($Z = 64$ m), lower ($Z = -64$ m), rear ($Y = 64$ m) and front ($Y = -64$ m) boundaries are no-flow/no-diffusion boundaries. The resulting flow field has a spatially uniform mean component parallel to the no-flow/no-diffusion boundaries. The permeability field K is a stationary random field, lognormally distributed and spatially correlated (Fig. 1a). We define $Y = \ln(K)$, where K is the permeability (expressed in [m/s]) and ln is the natural logarithm. The Y field was generated using a spectral method (Dietrich and Newsam, 1993), using an isotropic exponential covariance model C_{YY}, with a correlation length $\lambda = 5$ m. To illustrate the effect of heterogeneity on solute transport, we tested two different values of variance: $\sigma_Y^2 = 2$ and $\sigma_Y^2 = 8$. The geometric mean of the field is $K_G = \exp(-9)$ m/s.

At the field scale, multiple geologic materials are typically encountered and, most of the time, the assumptions of stationarity, constant porosity and the use of very simple initial and boundary conditions would not be adequate. However, in a field problem, major hydrogeologic units can usually be mapped with a reasonably low uncertainty, and can be incorporated into a numerical model for groundwater flow. We therefore consider here the problem of solute transport over a finite distance, through a single hydrogeologic unit with a constant mean hydraulic conductivity and a certain level of intrinsic variability. We adopted a very common model for heterogeneity, usually suited to describe the natural variability of unconsolidated geological material.

It appears that the correlation and the variance values used in this study are in the range of other recent numerical studies. For example, Salandin and Fiorotto (1998) investigated flow and transport in two-dimensional synthetic aquifers with correlation lengths being 2–8 times the grid size and variances between 0.05 and 4. Trefry et al. (2003) performed two-dimensional transport simulations in isotropic log-Gaussian permeability fields with similar structural parameters, over a larger domain (up to 1024 times the correlation length in the longitudinal direction). Large three-dimensional synthetic aquifers were investigated by Jankovic et al. (2006) for variance values between 2 and 8.
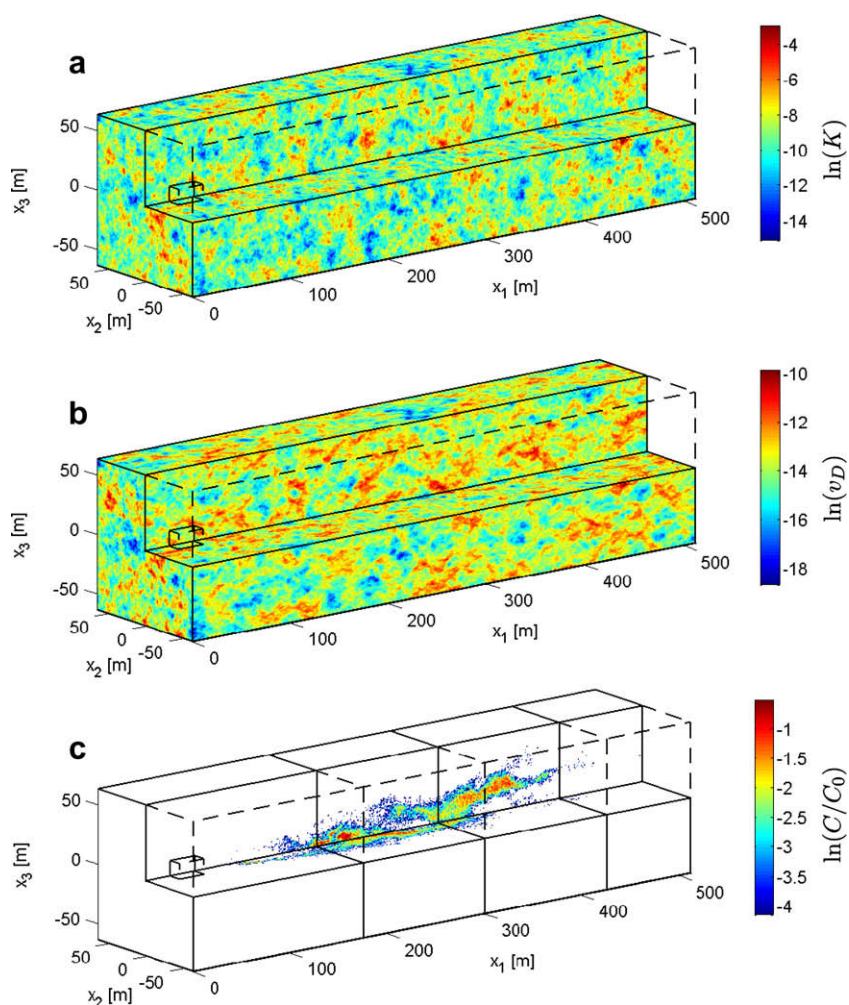
Figure 1 Reference example – case $\sigma_Y^2 = 2$. (a) Log-permeability field. (b) Logarithm of Darcy velocity v_D. (c) Snapshot of the plume (logarithm of the relative concentration) at time $t = 500$ days. The small cube located in the upstream zone delineates the injection zone. Control planes for reference breakthrough curves (BTC's) are also shown.
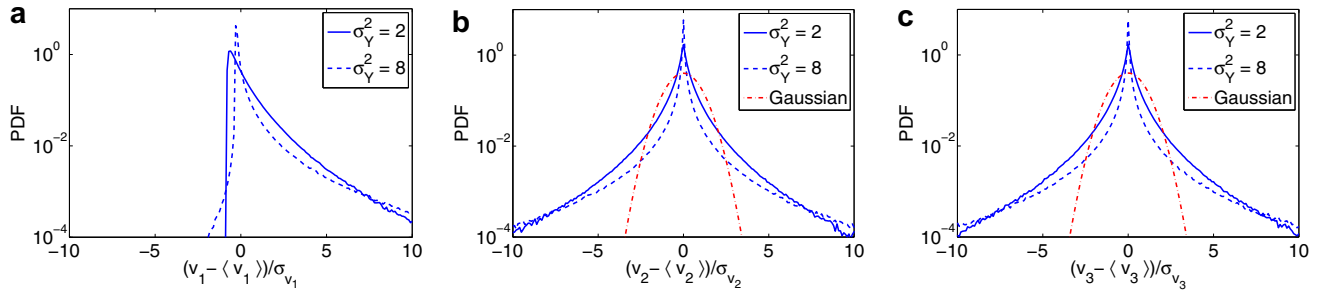
Figure 2 Comparison of probability density functions (PDF's) of Darcy velocity components for $\sigma_Y^2 = 2$ and $\sigma_Y^2 = 8$. Ideal Gaussian distributions are also drawn for comparison with transverse velocity probability density functions.

Flow was solved using the block-centered finite-difference code MODFLOW 2000 (Harbaugh et al., 2000). Even for $\sigma_Y^2 = 2$, the velocity field exhibits preferential pathways and more stagnant zones (Fig. 1b). Fig. 2 shows the velocity distributions. The results exhibit trends similar to what Trefry et al. (2003) obtained using two-dimensional simulations. The peak of the longitudinal velocity distribution becomes sharper as variance increases, and the apparent curvature of the distribution is turned upward. The heavy tails of the high-variance-case distribution might also announce anomalous transport. Transverse velocity distributions have a shape comparable to the distributions of Trefry et al. (2003).

Effective permeability was obtained from the computed total discharge through the domain, using Darcy's law and the gradient imposed at boundaries. Table 1 summarizes the values of effective permeability and velocity variances. The literature on upscaling of flow in heterogeneous media is very abundant. We simply refer the reader to the review of Wen and Gomez-Hernàndez (1996) and apply here basic results from stochastic flow theories. For a 3D isotropic medium, the theoretical effective permeability is $K_{e,th} = \gamma \times K_G$ (Gelhar, 1993). $\gamma = \exp(\sigma_Y^2/6)$ is the flow factor introduced by Gelhar and Axness (1983) to account for flow dimensionality. In this case, it appears that taking $\gamma = 1$, as advised by Dagan (1989), yields a higher discrepancy between the observed K_e and its theoretical value. The variance of the velocity components are $\sigma_{v_1,th}^2 = 8\sigma_Y^2 K_g^2 J^2/15$ and $\sigma_{v_2,th}^2 = \sigma_{v_3,th}^2 = \sigma_Y^2 K_g^2 J^2/15$ (Gelhar, 1993). If a correct order of magnitude is predicted for the case $\sigma_Y^2 = 2$, classical stochastic theories totally underestimate velocity variance values for the case $\sigma_Y^2 = 8$.

Transport was solved using the particle-tracking code RWHet (Labolle, 2000). Initial concentration is null everywhere. 1,000,000 particles are released instantaneously at time $t = 0$. The particles are spread uniformly over a cubic region of $5\lambda \times 5\lambda \times 5\lambda$ (Fig. 1), yielding an initial concentration C_0 of 64 particles per cell. The injection zone is centered on the longitudinal axis of the domain and located at a distance 5λ downstream of the upstream fixed-head boundary. The clear distance to upper, lower, rear and front boundaries is 10.3λ. Boundary effects should therefore be kept to a minimum (Bellin et al., 1992; Rubin and Dagan, 1988, 1989). Due to the limited extent of the source, it is also expected that the plume does not sample the full heterogeneity of the aquifer. Local (or microscopic) longitudinal and transverse dispersivities are set equal to 0.1 m and 0.01 m, respectively. The effective diffusion coefficient is $D^d = 10^{-9}$ m^2/s. Typically, such local processes are not considered when performing numerical simulations of solute transport in heterogeneous media. However, as already stated, the goal of these simulations is not to focus on some idealized situation in which one of the models will perform best, but rather be representative of a simplified but realistic field situation.

The porosity is assumed to be constant and equal to $\theta = 40\%$. The corresponding average longitudinal and transverse grid Peclet numbers are respectively equal to $P_{e,L} = v\Delta L/D_L \approx \Delta L/\alpha_L = 10$ and $P_{e,T} = v\Delta L/D_T \approx \Delta L/\alpha_T = 100$, v being a characteristic mean velocity. Even at a lower variance, the resulting solute plumes are relatively elongated and distorted (Fig. 1c). However, we will show that, for $\sigma_Y^2 = 2$, cumulative breakthrough curves at control planes have a Gaussian shape, which could make the use of macro-dispersion theories more suited to this situation. We will also show that cumulative breakthrough curves become more distorted as variance increases, as a result of the higher variability of the velocity field and as a result of diffusive mass exchange between zones of high and low velocity.

Upscaling methods for longitudinal dispersivity

In a general stochastic framework, statistics of output variables (e.g. concentration distributions) are drawn from the statistics of input variables (e.g. hydraulic conductivity distributions). Monte Carlo simulations are the most general tool to establish the link between input and output variables, especially when they are nonlinearly related. The approach consists in generating a large number of statistically

Table 1 Effective permeability, statistics of the flow field, and corresponding theoretical values from stochastic models

	$\sigma_Y^2 = 2$	$\sigma_Y^2 = 8$
K_e (10^{-4} m/s)	1.575	3.276
$K_{e,th}(\gamma = \exp(\sigma_Y^2/6))$ (10^{-4} m/s)	1.722	4.682
$K_{e,th}(\gamma = 1)$ (10^{-4} m/s)	1.234	1.234
$\sigma_{v_1}^2$ (10^{-12} m^2/s^2)	3.554	137.3
$\sigma_{v_1,th}^2$ (10^{-12} m^2/s^2)	1.625	6.498
$\sigma_{v_2}^2$ (10^{-13} m^2/s)	6.914	518.5
$\sigma_{v_3}^2$ (10^{-13} m^2/s)	7.556	575.5
$\sigma_{v_2,th}^2 = \sigma_{v_3,th}^2$ (10^{-13} m^2/s^2)	2.031	8.123

equivalent sets of input variables, and explicitly solve the problem of interest to obtain a set of output variables. However, the focus of the paper is on analytical and semi-analytical models for solute transport, and Monte Carlo methods will not be further reviewed here.

Historically, one of the first stochastic method applied to study field-scale solute transport under heterogeneous conditions is the stochastic-convective method (Dagan and Bresler, 1979; Simmons, 1982; Sposito et al., 1986). The tracer is divided into a finite number of particles, being transported along their own path according to some velocity (Simmons et al., 1995). Typically, the velocity distribution is assigned a probability density function, where any velocity realization is assigned a probability. The main assumption is that particles on a streamline do not interact at all with particles on other streamlines. Stochastic-convective models are therefore also referred to as stochastic streamtube models. This class of stochastic methods is mostly suited to the modeling of transport in the vadose zone, where solute migration mainly occurs in the vertical direction (Dagan and Bresler, 1979). Applications in the saturated zone have also been reported for reactive transport (Ginn, 2001; Luo et al., 2006). Since these methods do not provide any quantitative description of solute plumes, but are instead restricted to the prediction and analyses of breakthrough curves, they will not be further described either.

Instead, we will focus here on stochastic perturbative methods, which represent the broadest category of stochastic models. These methods involve small-scale fluctuations of random input and output variables, linked in an analytical framework through first-order (or higher-order) approximations. A heterogeneous permeability field is viewed as one realization of a spatial multidimensional random process, characterized by a mean, a variance and a covariance function (Gelhar, 1993). The permeability field also has to fulfill stationarity and ergodicity. Stationarity implies that there is no spatial trend in the permeability and that the correlation length is constant. Ergodicity implies that all states present in all possible statistically equivalent realizations are represented in the single realization of interest. This latter property allows ensemble-averaging over all realizations to be equivalent to spatial averaging over one single realization. Finally, the hydraulic conductivity is usually assumed to be lognormally distributed. This assumption has the advantage that negative values are excluded, which is consistent with the physical requirement that permeability is positive (Gelhar, 1993). Although field distributions of hydraulic conductivity are not necessarily lognormal, such distributions have been observed, e.g. by Sudicky (1986) for the Borden aquifer, or by Hess et al. (1992) for the Cape Cod aquifer.

Three main stochastic approaches are reported in this section, each corresponding to a particular type of heterogeneity. First, the ''classical'' stochastic theory focuses on lognormally distributed permeability fields characterized by covariance models having finite correlation lengths. This theory is referred to as the classical stochastic model, because it builds upon the original and pioneering works of Gelhar et al. (1979), Gelhar and Axness (1983) and Dagan (1984). Since the literature in this domain is relatively abundant (see the textbooks of Dagan (1989), Gelhar

(1993) or Rubin (2003)), this paper does not fully detail the approach. Instead, the emphasis is placed on one of the major contributions in the domain: the Eulerian derivation of macrodispersion by Gelhar and Axness (1983). In section ''Extension to fractal permeability fields'', the ''classical'' stochastic approach is extended to account for permeability fields characterized by algebraic covariance models, corresponding to fractal permeability fields (Zhan and Wheatcraft, 1996). Both finite correlation length models and fractal models have also been reviewed by Vogel and Roth (2003). Finally, models adapted to permeability fields having a discrete and/or a multimodal distribution are presented in section ''Inclusion models''. Although the latter category of models can virtually mimic any two-point covariance model (Dagan et al., 2003), their most straightforward application is transport through media composed of inclusions of given shapes and permeabilities, with a discrete permeability distribution. In this work, these models are referred to as ''inclusion models''.

The ''classical'' stochastic approach

Stochastic pertubative models are based on a small perturbation approach. Variables of interest are split into a constant mean (bracketed value $\langle \rangle$) and a zero-mean random perturbation (marked value $'$), caused by the variability in the permeability field. In an Eulerian framework, concentration and velocity are the variable of interest and are expressed as (Gelhar and Axness, 1983)

$$
\begin{aligned}
C &= \langle C \rangle + C', \\
v &= \langle v \rangle + v
\end{aligned}
\tag{7}
$$

Substituting (7) into the advection—dispersion equation and taking expected values leads to a governing equation for the mean concentration $\langle C \rangle$

$$
\frac{\partial \langle C \rangle}{\partial t} + \sum_i \langle v_i \rangle \frac{\partial \langle C \rangle}{\partial x_i} - \sum_i \sum_j \frac{\partial}{\partial x_i} D_{ij}^H \frac{\partial \langle C \rangle}{\partial x_j}
$$
$$
= -E\left[\sum_i v_i' \frac{\partial C'}{\partial x_i} \right]
\tag{8}
$$

where $E[\,]$ is used as an alternative notation to $\langle \rangle$. Eq. (8) is similar to (2), except that a second-order term arises here. It reflects additional mass transport due to correlation between specific discharge and concentration fluctuations. It produces a large-scale dispersion effect and can be approximated using a Fickian-like law (Gelhar and Axness, 1983)

$$
E\left[\sum_i v_i' \frac{\partial C'}{\partial x_i} \right] = \sum_i \frac{\partial}{\partial x_i} \langle v_i' C' \rangle
$$
$$
\approx -\sum_i \sum_j \frac{\partial}{\partial x_i} \left(D_{ij}^* \frac{\partial \langle C \rangle}{\partial x_j} \right)
\tag{9}
$$

The macrodispersion tensor D_{ij}^* is proportional to the absolute value of migration velocity, as for the local dispersion tensor (Gelhar and Axness, 1983). D_{ij}^* can be evaluated from (9) using the governing equation of concentration perturbations. The latter is obtained by subtracting (8) from the original governing equation of C, which yields

$$\frac{\partial C'}{\partial t} + \sum_i \left(v_i' \frac{\partial \langle C \rangle}{\partial x_i} + \langle v_i \rangle \frac{\partial C'}{\partial x_i} \right) - \sum_i \sum_j \frac{\partial}{\partial x_i} \left(D_{ij}^H \frac{\partial C'}{\partial x_j} \right)$$

$$= \sum_i \frac{\partial}{\partial x_i} \left(v_i' C' - \langle v_i' C' \rangle \right) \approx 0 \tag{10}$$

The approximation in (10) is of crucial importance. It implies that velocity fluctuations are sufficiently small for second-order products to be neglected. For a lognormal permeability field, it can be shown based on a similar stochastic analysis of the flow equation that this condition on velocity perturbation requires a small variance of the Y field, so that it can be linearized (Gelhar, 1993).

In general, (8) and (10) must be solved simultaneously. However, a decoupling can be accomplished provided that concentration fluctuations occurs at a much smaller scale than variations associated to the mean concentration (Gelhar, 1993). It is then possible to solve (10) to evaluate the macrodispersive flux and subsequently substitute it in (8). In the particular case of a mean flow occurring in direction $i = 1$, Gelhar and Axness (1983) showed using Fourier-transform techniques that in the lowest order perturbation theory, $\alpha_L^* = D_{11}^*/\langle v_1 \rangle$ can be computed as

$$\alpha_L^*(t) = \int \frac{1 - \exp(-b \langle v_1 \rangle t)}{\gamma^2 b} \left(1 - \frac{s_1^2}{s^2} \right)^2 S_{YY}(\mathbf{s}) d\mathbf{s} \tag{11}$$

where $b = 2\pi i s_1 + 4\pi^2 \alpha_L s_1^2 + 4\pi^2 \alpha_T (s_2^2 + s_3^2)$ and $\mathbf{s} = (s_1, s_2, s_3)$ are the Fourier coordinates. S_{YY} is the density spectrum of the log-permeability field. $S_{YY} = \mathscr{F}(C_{YY})$ is the Fourier transform of the log-permeability covariance function. Eq. (11) establishes the link between log-permeability fluctuations and macrodispersivity. Macrodispersivity is basically found to be dependent on the level of heterogeneity of the subsurface.

Moreover, macrodispersivity is also proved to be time-dependent and, as the exponential term in (11) vanishes for large time, provided the velocity spectrum is bounded, macrodispersivity converges to a constant asymptotic value. These are important features of solute transport in heterogeneous formations that are statistically homogeneous. In the preasymptotic regime, since α_L^* increases with time, the dispersive flux is not Fickian. In other words, the advection-dispersion equation is not an appropriate model for solute transport at early times. Second, provided that the velocity field has a bounded spectrum, solute transport is expected to become Fickian in the long time limit. The travel distance needed to reach this asymptotic behavior is usually of the order of tens of horizontal correlation lengths (Dagan, 1988).

Eq. (11) requires that ergodic conditions are fulfilled. This implies that solute plumes sample the full distribution of velocities in the aquifer. In the case of a source zone of a small size compared to correlation length, solute plumes do not experience the full variability of the aquifer. Hence, effective dispersion coefficients not only depend on the scale of heterogeneities, but also depend on the scale of the plume itself (Rajaram and Gelhar, 1993). Solute plumes originating from sources of finite size are therefore expected to be characterized by lower dispersion coefficients than predicted by (11) (Attinger et al., 1999; Dagan, 1990; Dentz et al., 2000a; Dentz et al., 2000b; Rajaram and Gelhar, 1993).

Finally, we mention that similar derivations of macrodispersivities were performed by other authors. Dagan (1984, 1988, 1989) used a Lagrangian framework, but had to use an approximate relationship between the Eulerian and the Lagrangian velocity covariance. Neuman et al. (1987) used a more abstract mathematical analysis based on semigroup theory. Basically, classical stochastic perturbative approaches to derive macrodispersivity values all require an assumption of relatively small perturbations, leading to little discrepancy among them and a domain of validity $\sigma_Y^2 < 1$ (Gelhar, 1993).

Extension to fractal permeability fields

Fractal geometry was initially introduced in the field of hydrogeology in the framework of streamtube models (Wheatcraft and Tyler, 1988; Zhou and Selim, 2002). Particle paths are described as fractal lines, and the resulting variability in travel times allows longitudinal dispersivity to become time- or space-dependent. However, the use of fractal geometry in subsurface hydrology expanded, based on the observation that pore space distributions and, more generally, log-permeability distributions happen to be self-similar (Adler, 1996; Molz and Boman, 1995; Molz et al., 2004; Muller, 1996; Pachepsky and Timlin, 1998; Painter, 1996; Tennekoon et al., 2003). An object is said to be self-similar when it can be subdivided in parts, each of which being (at least approximately) a reduced copy of the whole (Mandelbrot, 1983). For such an object, it is not possible to identify a single characteristic length. Self-similarity is therefore linked to the concept of scale invariance.

An example of fractal model of heterogeneity is the fractional Brownian motion (fBm). A fBm is a non-stationary stochastic process and is defined through its increments. For example, a one-dimensional fBm $m(x)$ (x being the spatial coordinate) is defined using $n(x, h) = m(x + h) - m(x)$. The increments $n(x, h)$ have a Gaussian distribution, with a zero mean and a variance σ^2. Moreover, $n(x, h)$ has to be statistically invariant with respect to an affine transformation (Molz et al., 1997). This latter property implies that $n(x, rh)$ and $r^H n(x, h)$ have the same Gaussian distribution, with a zero mean and a variance $r^{2H} \sigma^2$ (Molz et al., 1997). It also follows from these properties that the semi-variogram of $m(x)$ follows a power law of the type $\sigma^2 h^{2H}$ (Fig. 3). The variable $n(x, h)$ that had to be defined to characterize $m(x)$ is another fractal model of heterogeneity: the fractional Gaussian noise (fGn). H is the so-called Hurst coefficient. Its value is bounded according to $0 < H < 1$. It is used to define the fractal dimension of an object $d_f = 1 + d_e - H$ (d_e being the Euclidian dimension). $H = 1$ corresponds thus to a non-fractal medium. A power-law variogram does not converge to a threshold value. The apparent correlation length is therefore infinite. Similarly, it can be shown that the variogram of a fGn exhibits much larger correlations than exponential or Gaussian variogram models.

The fractal Lévy-stable motion (fLm) is a third noteworthy fractal model, based on non-Gaussian distributions called Lévy distributions (Lévy, 1937; Molz et al., 1997; Painter and Paterson, 1994). Such probability distributions will be further presented in section ''CTRW and frac-
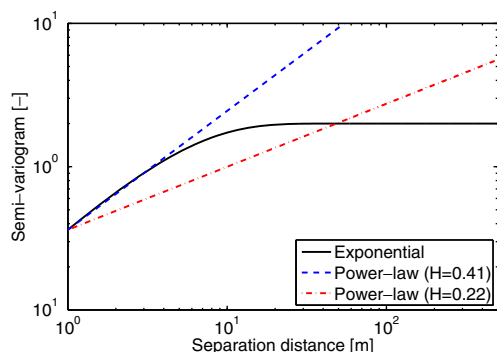
Figure 3 Comparison of fractal fBm semi-variograms with the theoretical exponential model adopted for the reference example (case $\sigma_Y^2 = 2$).

tional-order PDE's''. One should also mention multifractal models of heterogeneous log-permeability fields. The fields do not scale according to a single Hurst coefficient anymore, but can be properly scaled by a variety of H values (Liu and Molz, 1997; Tennekoon et al., 2003). On a log–log scaled graph, a monofractal power-law covariance function plots as a straight line (Fig. 3), while multifractal structure functions usually exhibit a curvature. In order to simulate long-range correlation, Rajaram and Gelhar (1995) also proposed to use a multiscale exponential model.

Apparent longitudinal dispersivities can be computed using the tools initially developed within the framework of stationary stochastic processes, using the appropriate variogram model. In the case of fractal heterogeneity, as correlation persists over a wide range of spatial scales, Fickian solute transport behavior will never be achieved, and apparent longitudinal dispersivity will monotonically increase with plume scale to infinity (Bellin et al., 1996; Neuman, 1995). However, for most geological formations, physical boundaries exist. When substituting the appropriate spectrum of the fractal log-permeability field into (11), cutoff frequencies have to be introduced to account for characteristic spatial scales of the problem and force apparent dispersivity to eventually converge to a constant macroscale value (Di Federico and Neuman, 1998; Hassan et al., 1997; Kemblowski and Wen, 1993). For example, Zhan and Wheatcraft (1996) derived analytical expressions for apparent dispersivity in fBm $\ln(K)$ fields using L_{max}, defined as the smallest distance to a no-flow boundary. The corresponding analytical solution will be illustrated for the reference examples.

Inclusion models

Transport in aquifers made of inclusions of highly contrasted permeabilities has only been more recently investigated. Desbarats (1990) performed pioneering numerical simulations using a binary medium with inclusions of low permeability and showed that permeability contrast and inclusion volumetric proportion were the main controlling parameters for transport. Rubin (1995) proposed a first-order stochastic approach and derived analytical results in the case of bimodal isotropic media, extended to anisotropic situations by Stauffer and Rauber (1998). Like other

results from stochastic theories, these results are only valid for low permeability contrasts. Eames and Bush (1999) and later Dagan and Lessoff (2001) and Lessoff and Dagan (2001) studied transport properties of two- and three-dimensional bimodal fields composed of inclusions of fixed size and of constant permeability, positioned at random in an homogeneous matrix. Their developments were conducted under the assumption of low volumetric proportion of inclusions (i.e. in the dilute system limit) so that advective transport could be solved by isolating one inclusion and the dispersive effect of a collection of lenses was determined subsequently in a simple additive manner.

Dagan et al. (2003) and Fiori et al. (2003a, 2006) further refined the analysis by considering distributions of blocks of different size and of different permeabilities. Dagan et al. (2003) suggested to model heterogeneous formations as multiphasic ones, made up of M types of block geometry and of N different types of material (Fig. 4a). Blocks are assumed not to overlap. A point of the medium lies in the block i, j of shape i ($i = 1, \ldots, M$) and of material j ($j = 1, \ldots, N$) with a known probability p_{ij}. p_{ij} thus denotes the volumetric proportion of blocks of size i and of material j in the medium. Centroid positions of blocks $\bar{\mathbf{x}}_{ij}$ are however not known and are treated as random variables. If K_j is the permeability of material j, the overall conductivity field is given by (Dagan et al., 2003)

$$K(\mathbf{x}) = \sum_i \sum_j K_j I(\mathbf{x} - \bar{\mathbf{x}}_{ij}) \tag{12}$$

where the indicator function $I(\mathbf{x} - \bar{\mathbf{x}}_{ij})$ is equal to 1 for $\mathbf{x}$ belonging to the inclusion (i, j) and is equal to zero otherwise. It is emphasized that permeabilities of two neighboring blocks remain uncorrelated. Mean and variance of the log-permeability field can be computed from

$$\ln(K_g) = \sum_i \sum_j p_{ij} Y_j \tag{13}$$

$$\sigma_Y^2 = \frac{1}{2} \sum_i \sum_j \sum_{k \neq j} (Y_j - Y_k)^2 p_{ij} p_{ik} \tag{14}$$

where $Y_j = \ln(K_j)$. It appears from (14) that the variance of such media can be very high, well above the classical limit $\sigma_Y^2 < 1$ established for the validity of first-order stochastic theories. To further simplify the model, Dagan et al. (2003) proposed to represent blocks as inclusions of regular size, such as ellipses or ellipsoids, and to assume that they are submerged in a matrix of arbitrary conductivity K_0 (Fig. 4b). In a given heterogeneous formation of this geometry, the solution of the flow field can be represented as a distribution of singularities of source type, each source corresponding to a given block. The self-consistent approach proceeds by isolating one inclusion of shape i and permeability K_j and by suppressing the remaining ones in the matrix of permeability K_0. The flow and transport problems are then solved assuming there is no interaction between each block (Fig. 4c). As K_0 could be any reference permeability somehow linked to the effective permeability K_e of the medium, the self-consistent approach assumes $K_0 = K_e$ and K_0 reflects the presence of the neighborings blocks that have been suppressed. The derivation of K_e for two- and three-dimensional isotropic media is given by Dagan (1979) and extended to three-dimensional anisotropic media in his textbook (Dagan, 1989).
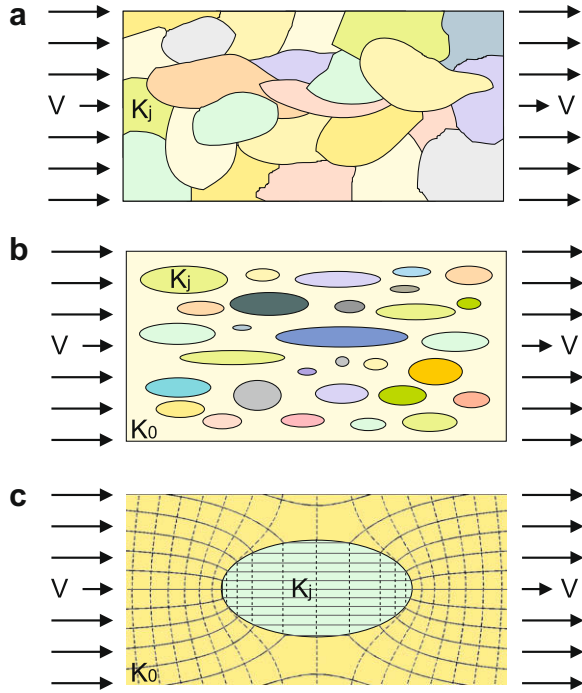
Figure 4 Conceptual aquifer model and the self-consistent approximation (in the 2D case). (a) Statistically homogeneous but anisotropic heterogeneous permeability field. (b) Model of inclusions of regular shape disposed at random in a matrix. (c) Single inclusion embedded in a matrix. Adapted from Dagan et al. (2003).

Under ergodic condition, the spatial moments of a solute plume can be computed from the statistical moments of the trajectory of a single particle. We consider a solute particle injected at time $t = 0$ and at position $\mathbf{x}_0$. The trajectory of this particle is $\mathbf{x} = \mathbf{X}(t, \mathbf{x}_0)$ and is given by (Dagan et al., 2003)

$$\mathbf{X}(t, \mathbf{x}_0) = \mathbf{x}_0 + \mathbf{V}t + \sum_i \sum_j \mathbf{X}'_{ij} \tag{15}$$

where $\mathbf{V}$ is the far field velocity and $\mathbf{X}'_{ij}$ is the trajectory fluctuation caused by block (i,j). The second moments of trajectories are given by (Dagan et al., 2003)

$$X_{11}(t) = \sum_i \sum_j E\left[X'_{ij,1}(\mathbf{x}_0 - \overline{\mathbf{x}}_{ij}) X'_{ij,1}(\mathbf{x}_0 - \overline{\mathbf{x}}_{ij}) \right] \tag{16}$$

where subscript 1 refers to the fluctuations along the longitudinal trajectory.

Following the work of Dagan et al. (2003), we further consider the continuous limit for permeability and for inclusion size. The volumetric proportion of blocks of size i and of material j tends to $p_{ij} \to pf(K, A)dKdA$. $p = \sum_i \sum_j p_{ij} \leqslant 1$ is the total volumetric proportion of inclusions and A is a characteristic size of inclusion (e.g. the longitudinal semi-axis). $f(K, A)$ is the joint distribution of permeability and ellipse size. It is assumed that the anisotropy ratio is identical for each inclusion. In that case, (16) can be transformed into (Dagan et al., 2003)

$$X_{11}(t) = p \int \frac{X'^2_1(t, \mathbf{x}_0, K, A)}{V(A)} f(K, A) d\mathbf{x}_0 \, dK \, dA \tag{17}$$

where $V(A)$ is the volume occupied by the ellipse of size A. In (17), integration is performed over all possible initial positions, i.e. $-\infty < x_{10} < \infty$, $-\infty < x_{20} < \infty$ and $-\infty < x_{30} < \infty$. Here, x_{10}, x_{20} and x_{30} are initial position coordinates. The longitudinal apparent dispersivity is computed from (Dagan et al., 2003)

$$\alpha_L^*(t) = \frac{1}{2V} \frac{dX_{11}(t)}{dt} \tag{18}$$

At the limit for $t \to \infty$, α_L^* converges to a constant value (Dagan et al., 2003)

$$\alpha_L^*(\infty) = \frac{p}{2} \int \frac{X'^2_1(\infty, (-\infty, x_{20}, x_{30}), K, A)}{V(A)} f(K, A) dx_{20} \, dx_{30} \, dK \, dA \tag{19}$$

Analytical solutions for flow past a single ellipse of radius A and permeability K embedded in a homogeneous medium of permeability K_e (Fig. 4c) are given, e.g. by Dagan (1979, 1989), Dagan and Lessoff (2001), and Fiori et al. (2003a). The solution of (19) for the reference example is illustrated in the following section.

Numerical studies have shown that the self-consistent approach could be reasonably used to compute apparent longitudinal dispersivity for solute transport in bimodal isotropic permeability fields, for volumetric proportions of inclusions ranging from 5% to 40% and for permeability ratios ranging from 0.01 to 10 (Fiori et al., 2003b; Jankovic et al., 2003a,b). Recent studies by Fiori et al. (2006) and Jankovic et al. (2006) also demonstrated the good performance of the self-consistent approach for solute transport in three-dimensional isotropic lognormal permeability fields with a variance going up to 8. It should finally be mentioned that Dagan and Fiori (2003) and Fiori and Dagan (2003) studied transport properties of media with composite inclusions, that allowed them to derive results without relying either on the dilute system assumption, or on the self-consistent approach. The analytical solutions of the corresponding velocity field are however more complicated, without bringing a significant modeling improvement (Jankovic et al., 2003b), which makes the self-consistent approach more appropriate.

Application to the reference example

Spatial moments of solute plumes are widely used to estimate apparent transport parameters (Trefry et al., 2003). As each particle carries the same mass of tracer M, zeroth-, first- and second-order longitudinal spatial moments of the solute plume are computed according to

$$m_0(t) = MN \tag{20}$$

$$m_1(t) = M \sum_{n=1}^{N} X_1^n(t) \tag{21}$$

$$m_{11}^c(t) = M \sum_{n=1}^{N} \left(X_1^n(t) - \langle x(t) \rangle \right)^2 \tag{22}$$

where N is the number of particles, $X_1^n(t)$ is the longitudinal position of particle n and $\langle x(t) \rangle = m_1(t)/m_0(t)$ is the mean longitudinal position of the plume. Mean velocity and apparent longitudinal dispersivity are obtained from (Tompson and Gelhar, 1990)

$$\langle v_1(t) \rangle = \frac{m_1(t) - m_1(0)}{m_0(t)t} \tag{23}$$

$$\alpha_L^*(t) = \frac{m_{11}^c(t) - m_{11}^c(0)}{2\langle v_1(t) \rangle m_0(t)t} \tag{24}$$

Spatial moments can no longer be computed when particles have left the flow domain. Time histories of $\alpha_L^*(t)$ are therefore limited to about $t = 486$ days for the case $\sigma_Y^2 = 2$ and $t = 86$ days for the case $\sigma_Y^2 = 8$ (Figs. 5 and 6). These time scales correspond to travel distances of about 33 and 23 correlation lengths, respectively.

If we ignore issues of ergodicity and the inadequately high variance values, the application of results from the classical stochastic approach is relatively straightforward. The analytical solution of (11) corresponding to a three-dimensional isotropic exponential covariance model is (Dagan, 1984)

$$\frac{\alpha_L^*(t)}{\alpha_L^*(\infty)} = 1 - \frac{4}{\xi^2} + \frac{24}{\xi^4} - 8\left(\frac{1}{\xi^2} + \frac{3}{\xi^3} + \frac{3}{\xi^4}\right)\exp(-\xi) \tag{25}$$

where $\xi = \langle v_1 \rangle t / \lambda$ and the constant asymptotic value is given by

$$\alpha_L^*(\infty) = \sigma_Y^2 \frac{\lambda}{\gamma^2} \tag{26}$$

where γ is the flow-factor introduced previously. Although taking $\gamma \neq 1$ allowed a correct prediction of the effective permeability of the synthetic aquifer, setting $\gamma = 1$ allows a better match of the asymptotic apparent longitudinal dis-

persivity (Fig. 5). This is consistent with the results of Chin (1997), who tested first-order stochastic dispersion theories using three-dimensional simulations of flow and transport, for log-permeability variances between 0.5 and 1.5. Preasymptotic transport is difficult to predict, due to ergodicity requirements that cannot be fulfilled at early times.

It could be argued that results from fractal theories cannot be applied to the reference examples used in this study, since the theoretical assumptions underlying the fractal methods are not fulfilled. We adopt an approach similar to that of a field problem, and assume that the actual structure of the log-permeability field is not known. We characterize the latter using fractal methods in order to apply the corresponding theories. Two power-law approximations of the theoretical exponential covariance model are tested (Fig. 3). For the case $\sigma_Y^2 = 2$, $H = 0.41$ correspond to the small-scale structure of the log-permeability field, whereas $H = 0.22$ was obtained by least-square matching of the covariance function across the whole range of represented scales. Since the slope of the variogram at zero lag do not depend on the variance, only the large-scale average Hurst coefficient has to be recomputed for the case $\sigma_Y^2 = 8$. A value $H = 0.18$ is found. The method proposed by Zhan and Wheatcraft (1996) is illustrated here. They used a power-law fBm model for the semi-variogram of the log-permeability field, with a spectrum expressed as

$$S_{YY}(s) = \frac{\sigma_Y^2}{4\pi}(8 - 2d_f)\left(\frac{L_{max}}{2\pi}\right)^{2d_f-8}\frac{1}{(2\pi s)^{2H+d_e}} \tag{27}$$
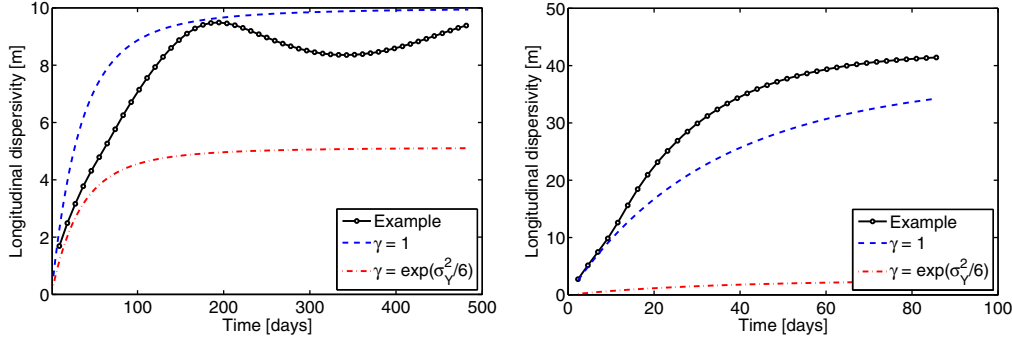
Figure 5 Comparison of the observed apparent longitudinal dispersivity with results from the classical stochastic upscaling method. Case $\sigma_Y^2 = 2$ (left), and case $\sigma_Y^2 = 8$ (right).
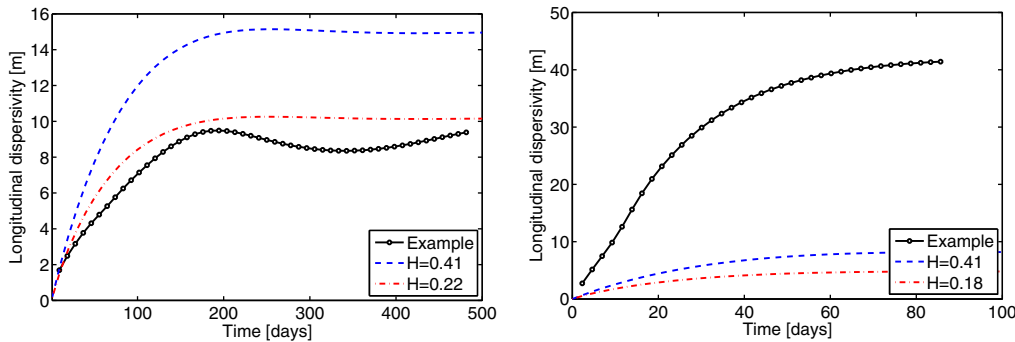
Figure 6 Comparison of the observed apparent longitudinal dispersivity with results from the fractal stochastic upscaling method (with $\gamma = \exp(\sigma_Y^2/6)$). Case $\sigma_Y^2 = 2$ (left), and case $\sigma_Y^2 = 8$ (right).

Eq. (27) was substituted into (11), which was then numerically integrated using a trapezoidal rule to compute the temporal development of macrodispersivity. As S_{YY} is not bounded for $s \to 0$, the integration is not performed over the whole frequency range. A minimum cutoff frequency $2\pi/L_{max}$ is introduced to account for model boundaries. Zhan and Wheatcraft (1996) advise to take the smallest model dimension for L_{max}. The computation was therefore performed with $L_{max} = 128$ m. One may however wonder if such a definition for L_{max} is appropriate, since the plume never reaches lateral model boundaries. For the case $\sigma_Y^2 = 2$, it appears that the fractal model corresponding to the whole range of spatial scales correctly predicts macrodispersivity, whereas the short-scale fractal model overestimates observed values (Fig. 6). For that case, taking a unit flow factor $\gamma = 1$ leads to important discrepancies between predicted and observed apparent longitudinal dispersivities. On the contrary, for the case $\sigma_Y^2 = 8$, both fractal models significantly underestimate apparent longitudinal dispersivity. Taking a unit flow factor value would lead both models to significantly overestimate α_L^*. The effective permeabilities adopted to compute $\langle v_1 \rangle$ in (11) are the theoretical values of 1.722×10^{-4} m/s and 4.682×10^{-4} m/s obtained from classical first-order stochastic theories. As these values only influence preasymptotic transport and do not influence constant macroscale values, it was not necessary to use fractal flow theories and compute actual theoretical fractal effective permeabilities.

Finally, inclusion models are applied by discretizing the Gaussian log-permeability distribution into a finite number of facies of constant permeability. The discrete PDF is computed by dividing the Y space into a finite number of bins of equal size. The center of bin i is the log-permeability Y_i of the corresponding facies. Facies proportions are computed from the mean of the PDF over each bin $p_i = \int_{bin} f(Y) dY$. We test three different discretizations: 3 bins, 5 bins, and 1001 bins. The latter case closely matches the full actual continuous PDF. It is therefore expected to yield to best upscaling results. Contrary to fractal models, the effective permeability explicitly appears in the computation of asymptotic macroscale longitudinal dispersivity. K_e has therefore to be computed according to the self-consistent approach. For a three-dimensional isotropic medium, K_e is obtained by solving (Dagan, 1989)

$$\int \frac{K_e - K}{2K_e - K} f(K) dK = 0 \qquad (28)$$

where $f(K)$ is the distribution of permeability. The results of the numerical integration of (28) for 3, 5 and 1001 facies are reported in Table 2. For the case $\sigma_Y^2 = 2$, the theoretical value matches the observed effective permeability closely, better than the prediction from the classical stochastic theory. The prediction of K_e for the case $\sigma_Y^2 = 8$ is lower than the actual value, but the error remains comparable to that of the classical stochastic theory. The covariance function corresponding to an isotropic multi-indicator permeability field with inclusions of constant size A has a correlation length $\lambda = 3A/4$ (Dagan et al., 2003). We compute the constant asymptotic longitudinal dispersivity by transforming (19) into (Dagan et al., 2003)

$$\alpha_L^*(\infty) = p \int \alpha_L^*(\infty, K, A) f(K) dK \qquad (29)$$

Table 2 Comparison of effective permeability and apparent longitudinal dispersivity with theoretical values derived from inclusion models

	$\sigma_Y^2 = 2$	$\sigma_Y^2 = 8$
K_e (10^{-4} m/s)	1.575	3.276
$K_{e,th}$ (3 facies) (10^{-4} m/s)	1.574	1.767
$K_{e,th}$ (5 facies) (10^{-4} m/s)	1.626	2.573
$K_{e,th}$ (1001 facies) (10^{-4} m/s)	1.589	2.574
α_L^* (m)	9.489	>41.41
$\alpha_{L,th}^*$ (3 facies) (m)	14.58	50.01
$\alpha_{L,th}^*$ (5 facies) (m)	12.77	63.09
$\alpha_{L,th}^*$ (1001 facies) (m)	10.89	54.47

Since convergence is not reached for case $\sigma_Y^2 = 8$, the largest numerical value of α_L^* is reported here, for comparison with asymptotic theoretical values.

where $\alpha_L^*(\infty, K, A)$ is the asymptotic longitudinal dispersivity associated with an inclusion of permeability K and radius A, embedded in a matrix of hydraulic conductivity K_e. In this work, we also used a cutoff permeability ratio of $K/K_e = 0.01$, in order to account for diffusion into low-permeability inclusions. Indeed, the theoretical dispersivity associated with inclusions of decreasing permeability grows without bounds (Dagan et al., 2003). However, at some point, we expect diffusion to play a role in transport through low-permeability inclusions. To account for this effect, we set $\alpha_L^*(\infty, K, A) = \alpha_L^*(\infty, K_e/100, A)$ for $K < K_e/100$ (Dagan et al., 2003). Decreasing the value of this cutoff permeability ratio would typically increase the value of macrodispersivity, by increasing $\alpha_L^*(\infty, K, A)$ for small K in (29). However, in this case, the probability of having $K/K_e < 0.01$ (i.e. the volumetric proportion of facies with $K/K_e < 0.01$) is relatively limited and the choice of the cutoff permeability is of little impact on the overall macrodispersivity value. Like the classical stochastic upscaling method, inclusion models are found to provide reasonable predictions of asymptotic macrodispersivity (Table 2). Even with a relatively high level of discretization of the log-permeability distribution (5 facies), a correct order of magnitude is reached.

We emphasize that the application reported here is rather simplified. Indeed, considering the relatively small source size and the limited extent of the domain, ergodicity is not likely to be fulfilled. The comparison of the numerical results with the semi-analytical solutions presented could therefore be highly questionable. Moreover, we only used semi-analytical results developed under an assumption of low variance. We recall that the reference examples have only an illustrative purpose, and are not specifically designed to validate the theories presented.

Nevertheless, for the case $\sigma_Y^2 = 2$, it appears that acceptable and comparable results in terms of apparent longitudinal dispersivity can be obtained based on any of the three characterizations of the aquifer tested here. The stochastic approach could be used with a relative confidence, since the theoretical variance and covariance function were known. Using a fractal approximation of the covariance function, we could also model the scale-effect in apparent dispersivity within reasonable errors bounds. However, we question

the estimation of the cutoff length scale L_{max}. The attempt to give a physical significance to this mathematical artifact does not seem to be convincing, since the plume never sampled such a lateral length scale. Inclusion models yielded results of a similar quality.

On the contrary, for the higher variance case, the classical stochastic approach could only yield satisfactory results provided that the appropriate flow factor γ was used, and the fractal model yielded poorer results. Only inclusion models could yield results of a quality similar to case $\sigma_Y^2 = 2$. Therefore, these models could provide an important alternative to first-order stochastic theories. Although we only computed here the constant asymptotic dispersivity, the approach makes it possible to predict the full time history of α_L^* from (18) (Fiori et al., 2003a). Moreover, inclusion models were recently used to compute full theoretical BTC's (Jankovic et al., 2006).

Further insights into practical applications of upscaling methods for dispersivity

The semi-analytical solutions reported in this section have mainly been used in the framework of theoretical or numerical studies, aimed at investigating the effect of physical heterogeneity on solute transport in highly conceptualized situations (e.g. Chin, 1997; Jankovic et al., 2006). Only in a very limited number of field examples, measurements were taken with the spatial resolution required to apply the solutions presented (Hess et al., 1992; Sudicky, 1986). In this section, we provide some insight into the practical applicability and limitations of upscaling methods for dispersivity in typical field situations.

The choice of the structural model for K lies at the heart of the estimation of apparent dispersion coefficients, and represent the major difference between the approaches presented in previous sections. In field applications, the choice of a structural model usually relies on a rather subjective choice. First, field data are usually not dense enough to fully support the assumption of a multi-Gaussian log-permeability field, as used for the reference example and as required by the classical stochastic method (Gomez-Hernàndez and Wen, 1998). Hence, the current trend in groundwater flow and transport modeling is to prefer geologic models in which hydraulic conductivity is not unimodal and continuously distributed, but rather binned into a finite number of discrete values. This type of model is further supported by the development of new tools permitting to directly characterize the structure of a finite number of facies from borehole log data (Carle and Fogg, 1996, 1997). In this framework, inclusion models introduced probably represent a more promising approach.

Secondly, whereas it is clear from Fig. 3 that the fit of a power-law model on the exponential variogram model is a bulk approximation, the noise in experimental data collected in the field is usually such that the choice of a single variogram model is not a straightforward task. However, it is also not likely that different models fitted on experimental data with a similar goodness-of-fit would produce significantly different results, as long as transport predictions are made on a spatial scale not exceeding the scale at which the variogram was established. On the contrary, when predic-tion are made outside of the range of the variogram, different structural models will have fundamentally different predictions. While the classical stochastic model and inclusion models will predict a convergence towards a constant asymptotic dispersion coefficient, fractal models will typically predict dispersion coefficients growing without bounds.

While we have only presented three types of models, other sub-scale geometric models have also been used in the literature. These other structural models have usually been used in the framework of large-scale Monte Carlo simulations, and have led to other theoretical results for averaged flow and concentration distribution behavior, in the absence of accompanying theories and analytical results. For example, Kohlbecker et al. (2006) characterized flow velocity distributions in fractal hydraulic conductivity fields. Similar work on three-dimensional fractal fields was also achieved by Doughty and Karasaki (2002). Benson et al. (2006) and Monnig et al. (2008) have simulated solute transport in anisotropic fractal hydraulic conductivity fields. Several other studies have focused on dispersion of solutes in heterogeneous fields created from indicator-based hydrofacies models (Lu et al., 2002; Sivakumar et al., 2005; Teles et al., 2004; Weissmann et al., 1999; Zappa et al., 2006).

The estimation of the structural properties of the hydraulic conductivity field requires that some a priori information is available. Typically, point measurements of hydraulic conductivity are available (Gomez-Hernàndez et al., 1997). When pumping tests and tracer tests are performed, inverse modeling can also be used to estimate the spatial distribution of K (Carrera and Neuman, 1986; Cirpka and Kitanidis, 2001; Harvey and Gorelick, 1995; Hendricks et al., 2003). Geophysical methods or other a priori knowledge can also be used in this framework, to constrain the distribution of hydraulic conductivity values (Chen et al., 2001; Hubbard and Rubin, 2000). If such data are available, it is not likely that semi-analytical solutions for longitudinal dispersivity are going to be used. Instead, numerical modeling using conditional or co-conditional realizations of the hydraulic conductivity field is performed to simulate flow and transport. In such conditional realizations, the uncertainty in subsurface properties is highly reduced at measurement locations, which can provide efficient constraints when the solute plume only samples a small part of the overall variability of the aquifer (i.e. in non-ergodic situations).

From a very practical point of view, the most likely common application of the upscaling methods for longitudinal dispersivity is the computation of block-effective values, accounting for subgrid variability in numerical models (Rubin et al., 1999). The typical scale of a numerical model for groundwater flow and transport is of the order of several tens to hundreds of square kilometers. Since most modelers do not use high performance computer clusters, but use personal computers, numerical grid cells have a size usually comprised between 10 and 100 m. The steady improvement in computer performance is not likely to yield a decrease in numerical grid size. The current trend is indeed to increase the complexity of the model, for example through a coupling with a surface water model and/or a climate model (e.g. Maxwell et al., 2007), rather than to improve the

spatial discretization. The application of upscaling methods for dispersivity at this scale is probably ideal since (1) it is unlikely that the variability of subsurface properties is very high at such scale, and (2) the corresponding correlation length is likely to be much smaller than the block size while source zones are typically larger, therefore ensuring ergodic conditions.

Upscaled transport equations

The advection—dispersion equation is not a valid model when concentration distributions are not Gaussian, which may occur in highly heterogeneous situations and at intermediate times (Jankovic et al., 2006). When the permeability ranges over multiple orders of magnitude in the same aquifer, diffusive processes dominate transport through very low permeability zones, and upscaled transport equations are needed to allow the modeling of the resulting skewed concentration distributions. The emphasis is put here on three categories of models. A first set of partial differential equations (PDE's) are obtained by augmenting the expression of the macroscale dispersive flux to account for additional features of the transport problem. For example, non-Fickian expressions for q^D can be obtained by explicitly solving the effect of small-scale heterogeneity on transport. Analytical solutions can be obtained in highly simplified situations, such as transport in perfectly stratified aquifers (Berentsen et al., 2005; Gelhar et al., 1979). Other approaches simply postulate non-Fickian constitutive relationships for the dispersive flux (Strack, 1992; Tompson, 1988).

The second category of transport models, Continuous Time Random Walk (CTRW) models are a generalization of Brownian motion for particle movements correlated in time or in space, that can yield fractional-order partial differential equations under specific conditions. Such models allow apparent dispersivity to vary in time or in space and feature skewed concentration distributions.

The third category of upscaled equations is commonly referred to as mobile—immobile models (MIM). The heterogeneous medium is divided into one mobile zone, where solutes undergo advection, dispersion and diffusion, and immobile zones, where advective transport is negligible. The advection-dispersion equation is augmented by sink/source terms accounting for mass transfer from/towards immobile regions. Exchange between mobile and immobile zones is quantified either using rate coefficients or using diffusion models. Whereas this type of model was developed to account for long tails and slowly converging concentration distributions, effective dispersion coefficients can be expressed in terms of MIM transport parameters (Valocchi, 1985) and simulations based on field-scale data showed that rate-limited models could correctly account for observed scale-effects in apparent dispersion (Feehley et al., 2000; Harvey and Gorelick, 2000). Although mult-irate mass transfer models were shown to be mathematically equivalent to temporal CTRW (Cvetkovic and Haggerty, 2002; Dentz and Berkowitz, 2003; Schumer et al., 2003a), MIM models will be presented in a separate section to preserve their specific mathematical formulations.

Although we are actually dealing with large-scale averaged concentrations (noted $\langle C \rangle$ in section ''Upscaling methods for longitudinal dispersivity''), the general notation C will adopted for concentration throughout this section.

Higher-order PDE's and telegraph equations

Historically, the first upscaling approaches were based on volume-averaging and mixture theory techniques. These were seen to complement the growing body of experimental results on flow and transport in porous media by providing theoretical links to fundamental results in hydrodynamics and mass transport mechanisms. Intrinsically, these models are not based upon any geometric model of the subscale medium. Rather, they rely on the postulation of constitutive relationships and their systematic simplification and parametrization to specific systems of interests. In this section, we focus on models having a direct practical applicability, i.e. models that can be formulated using simple partial differential equations. We do not present them in a chronological order, and we include in the review models based on specific geometric models of heterogeneity. We start by introducing higher-order PDE's, and show how they can reduce to telegraph equations in certain situations. Then we introduce two other models involving different telegraph equations.

Berentsen (2003) and Berentsen et al. (2005) studied solute transport in perfectly stratified media based on the approach developed by Camacho (1993a,b,c) for laminar flow between parallel plates. They obtained a non-Fickian relaxation equation for the macrodispersive flux using Fourier analysis to average the advection—dispersion equation

$$q^D = -\tau_e \sigma_v^2 \frac{\partial C}{\partial x} - \tau_e \frac{\partial q^D}{\partial t} - (1 + \gamma_a)\tau_e v \frac{\partial q^D}{\partial x} + \tau_e D^d \frac{\partial^2 q^D}{\partial x^2} \qquad (30)$$

where τ_e is an effective relaxation time characterizing exponential degradation towards Fickian behavior. σ_v^2 is the variance of the velocity profile and γ_a is linked to its skewness. D_d is the effective molecular diffusion coefficient. As stated in the introduction of this section, the notation C used here actually refers to an averaged concentration, noted $\langle C \rangle$ in previous sections. Incorporating (30) into the mass balance equation (1) leads to a fourth-order transport model that can account for molecular diffusion, macrodispersion due to transverse mixing in non-uniform one-dimensional flow fields and that can yield asymmetric concentration distributions

$$\frac{\partial C}{\partial t} = -v \frac{\partial C}{\partial x} + \left[D_L + \tau_e \left(\sigma_v^2 - (1 + \gamma_a)v^2 \right) \right] \frac{\partial^2 C}{\partial x^2}$$
$$- \tau_e \left[\frac{\partial^2 C}{\partial t^2} + (2 + \gamma_a)v \frac{\partial^2 C}{\partial x \partial t} \right]$$
$$+ D^d \tau_e \left[2 \frac{\partial^3 C}{\partial x^2 \partial t} + (2 + \gamma_a)v \frac{\partial^3 C}{\partial x^3} - \frac{\partial^4 C}{\partial x^4} \right] \qquad (31)$$

If the velocity distribution is symmetrical, γ_a is equal to zero. When molecular diffusion can be neglected while a significant transverse variation in the velocity field is present, (31) reduces then to a second-order telegraph equation

$$\frac{\partial C}{\partial t} = -v\frac{\partial C}{\partial x} + \left[D_L + \tau_e(\sigma_v^2 - v^2)\right]\frac{\partial^2 C}{\partial x^2} - \tau_e\frac{\partial^2 C}{\partial t^2} - 2\tau_e v\frac{\partial^2 C}{\partial x\partial t} \tag{32}$$

which was initially established by Scheidegger (1960) in a more general framework. Analytical solutions of (32) are given, e.g. by Berentsen (2003) and Scheidegger (1958). A noticeable feature of (32) is that theoretical concentration fronts have sharp cutoffs at tailing edges, which does not necessarily fit experimental results.

Gelhar et al. (1979) also studied solute transport in a perfectly stratified aquifer. Using a stochastic approach, an analytical solution for concentration fluctuations was obtained, which could be injected in the governing equation of the mean concentration. They truncated the latter to the third-order term, which resulted in

$$\frac{\partial C}{\partial t} = -v\frac{\partial C}{\partial x} + \left((\alpha_L^* + \alpha_L)v + D^d\right)\frac{\partial^2 C}{\partial x^2} - \gamma_G\frac{\partial^3 C}{\partial t\partial x^2} - \gamma_G v\frac{\partial^3 C}{\partial x^3} = 0 \tag{33}$$

where α_L^* and γ_G can be computed from a geostatistical characterization of the permeability profile. α_L^* is the macroscale longitudinal dispersivity.

The advection–dispersion equation is a parabolic differential equation. No downstream condition is needed for concentration whereas solute front velocity is theoretically infinite. After a small time step, concentration at infinity is non-zero. Regarding this physical inconsistency, Strack (1992) proposed to include an inertia term in the constitutive equation of the dispersive flux

$$q^D = -D_L\frac{\partial C}{\partial x} - \frac{\lambda_S}{v}\frac{\partial q_D}{\partial t} \tag{34}$$

where λ_S is a parameter having the dimension of a length. Strack (1992) found from experimental evidence λ_S to be inversely proportional to solute velocity. Incorporating this expression into (1) leads to an equation slightly different from the advection-dispersion equation and comparable to (32)

$$\frac{\partial C}{\partial t} = -v\frac{\partial C}{\partial x} + D_L\frac{\partial^2 C}{\partial x^2} - \frac{\lambda_S}{v}\left(v\frac{\partial^2 C}{\partial x\partial t} + \frac{\partial^2 C}{\partial t^2}\right) \tag{35}$$

Analytical solutions of (35) are given by Strack (1992). As for Scheidegger equation, theoretical solute fronts are characterized by a sharp leading edge, with the difference that late-time tails are smoothened. However, Strack (1992) indicates that the first and second temporal moments of (35) are similar to those of the advection-dispersion equation. Hence, Strack telegraph equation has no upscaling capacities with respect to dispersion.

Tompson and Gray (1986) used a volumetric averaging technique to derive large-scale balance equations. Their work was further simplified by Tompson (1988), who derived another relationship for the dispersive solute flux, the latter being written in the one-dimensional case as

$$q^D = -D_L\frac{\partial C}{\partial x} - \tau_e\frac{\partial q^D}{\partial t} - \tau_e v\frac{\partial q^D}{\partial x} \tag{36}$$

Tompson (1988) also derived a transport telegraph equation, which can be shown to be a generalization of (32), accounting for diffusion effects.

Hassanizadeh (1996) also used a volumetric averaging technique to scale up microscopic flow and transport equations. Solute dispersive flux was described using physical and chemical properties, such as chemical potentials or solute Helmholtz free energy. Hassanizadeh (1996) showed his model to be a more general form of Scheidegger, Tompson and Strack models. Most of other non-Fickian models are obtained by similar flow and transport upscaling technique, as reported from Whitaker by Peters and Smith (2000). Some of them are evoked by Hassanizadeh (1996), Maas (1999), Strack (1992), Tompson (1988), and Tompson and Gray (1986).

CTRW and fractional-order PDE's

The second category of model is based on the Continuous Time Random Walk approach. Recently, Berkowitz et al. (2006) have published a very detailed review of the application of CTRW for modeling non-Fickian transport in geological formations. Zhang et al. (2007b) have also recently published a review of space-fractional advection–dispersion equations, emphasizing on diverse available formulas, numerical solutions and an application to the MADE site data. In this section, we only present the basic aspects of the method and refer to the original papers, while more information and detailed applications of the method to field and laboratory situations can be found in Berkowitz et al.'s review (Berkowitz et al., 2006) and Zhang et al.'s paper (Zhang et al., 2007b).

Probabilistic models for solute transport
CTRW are a generalization of ordinary random walks (where the continuation of the walk occurs at discrete time steps) (Berkowitz and Scher, 1995). In a heterogeneous medium, solute particles are transported along different paths at varying velocities. Under ergodic conditions, this kind of transport can in general be represented using a coupled time-space probability density function $p(\mathbf{x}, t)$, describing particle transitions in space (jumps of varying length) and in time (waiting times between two successive jumps) (Benson, 1998; Berkowitz and Scher, 1995; Metzler and Klafter, 2000). The jump length PDF is $\phi(\mathbf{x}) = \int_0^\infty p(\mathbf{x}, t)\,dt$ and the waiting time PDF is $\psi(t) = \int_{-\infty}^\infty p(\mathbf{x}, t)\,d\mathbf{x}$.

The fundamental properties of transport are governed by the asymptotic behavior of $p(\mathbf{x}, t)$ (Berkowitz et al., 2001). Consider the case where jumps and waiting times are independent, i.e. $p(\mathbf{x}, t) = \phi(\mathbf{x})\psi(t)$. The term asymptotic behavior is used to refer to the long-distance (resp. long-time) behavior. A common asymptotic form of $\phi(\mathbf{x})$ (resp. $\psi(t)$) is the exponential decay ($\phi(\mathbf{x}) \rightarrow \exp(-\mathbf{x})$ or $\psi(t) \rightarrow \exp(-t)$). We define the ith statistical moment of jump and waiting time distributions according to $\mu_\phi^i = \int \mathbf{x}^i\phi(\mathbf{x})d\mathbf{x}$ and $\mu_\psi^i = \int t^i\psi(t)dt$, respectively. Adoption of exponential forms leads to all moments of $\phi(\mathbf{x})$ and $\psi(t)$ to be finite. In that case, according to the Central Limit Theorem, solute concentration distributions will eventually become Gaussian (Dentz and Berkowitz, 2003; Dentz et al., 2004; Trefry et al., 2003). The limit process for particle movement is then a Brownian motion governed by Fick's law (Baeumer et al., 2005). However, the movement of a particle in an aquifer generally does not follow uncorrelated

Brownian motion, since geological material is deposited in sequenced and correlated units. A particle traveling faster than the mean at some instant is much more likely to be still traveling faster at later times, due to spatial correlation in aquifer hydraulic conductivity (Benson et al., 2000b). This also means that particles traveling at velocities significantly different from the mean velocity may occur more often than Brownian motion can model (Benson, 1998; Schumer et al., 2001).

In the general CTRW framework, moving particles undergo random transitions according to a probability density function characterized by a different asymptotic form: the marginal PDF of the spatial (resp. temporal) random increments decays algebraically (i.e. according to a power law). This type of function is called a Lévy stable distribution, as they were first shown to exist by Paul Lévy (Lévy, 1937). For a PDF with tails falling off according to an algebraic-in-space decay $\phi(\mathbf{x}) \rightarrow |\mathbf{x}|^{-1-\beta_x}$, the variance of the jumps is infinite. In that case, transport is said to be spatially anomalous. Similarly, for a PDF with tails falling off according to an algebraic-in-time decay $\psi(t) \rightarrow t^{-1-\beta_t}$, the variance of the pausing times is infinite and transport is said to be temporally anomalous. β_x and β_t are positive numbers, since the integral of the probability density function must be finite. For $\beta_x \geqslant 2$ and $\beta_t \geqslant 2$, the first two spatial and temporal moments of $p(\mathbf{x}, t)$ exist and particles exhibit Gaussian behavior. If $1 < \beta_x < 2$, the second spatial moment of $p(\mathbf{x}, t)$ diverges. Similarly, if $1 < \beta_t < 2$, its second temporal moment diverges too. The cases $\beta_x < 1$ and $\beta_t < 1$ correspond to infinite mean jump and infinite mean pausing time, respectively.

For transport in heterogeneous media with highly conductive layers or fractures, the distribution of jump lengths is relatively broad, as particles may remain in low velocity channels whereas other particles travel at a velocity much higher than the mean. In that case, one could expect β_x to be lower than 2. Reciprocally, transport in a medium with low permeability inclusions could be characterized by $\beta_t < 2$, as particles captured in inclusions exhibit significantly longer pausing times (Meerschaert et al., 2002).

It must be noted that, in fact, β_x and β_t are functions of the length scale (or the time needed to traverse this length scale). The CTRW theory can be applied when β_x or β_t are constant or slowly varying over a number of orders of magnitude in length or in time (Margolin and Berkowitz, 2000). Geological systems can encounter heterogeneities over different hierarchical scales, and the characteristic length of the largest heterogeneity is likely to influence β_x and β_t the most (Margolin and Berkowitz, 2000). However, this largest heterogeneity must be small enough compared to the full travel distance of the particle cloud, so that the ergodic hypothesis is valid and probability distributions correctly approximate concentration distributions. If it is not the case, then large heterogeneities must be treated deterministically (Margolin and Berkowitz, 2000) or a characteristic scale for the largest heterogeneity must be included in the parametrization of $p(\mathbf{x}, t)$ (Dentz et al., 2004).

Mathematical formulations

First, we consider temporally anomalous transport ($\beta_x \geqslant 2$ and $0 < \beta_t < 2$). We define the Laplace transform of the waiting time PDF $\psi(u) = \mathscr{L}(\psi(t))$. Physical considerations limit the range of possible functional forms for $\psi(u)$. $\psi(u)$ must remain positive, normalized and bounded for all times (Cortis et al., 2004). Moreover, for applications to real systems, $\psi(u)$ and parameters values within it must be derived from measurable properties of the medium, the flow field or the tracer itself (Cortis et al., 2004). Dentz et al. (2004) introduced a truncated power law model for $\psi(u)$

$$\psi(u) = (1 + \tau_2 u t_1)^{\beta_t} \exp(t_1 u) \frac{\Gamma(-\beta_t, \tau_2^{-1} + t_1 u)}{\Gamma(-\beta_t, \tau_2^{-1})} \tag{37}$$

where $\tau_2 = t_2/t_1$ and $\Gamma(a, x)$ is the incomplete Gamma function (Abramowitz and Stegun, 1970). t_1 and t_2 have dimensions of time. For $t_1 \ll t \ll t_2$, $\psi(t) \rightarrow (t/t_1)^{-1-\beta_t}$. In this regime, transport behavior is anomalous (Cortis et al., 2004). For $t \gg t_2$, transport becomes Fickian for any β_t. The truncated power law model thus emphasizes the intermediate range algebraic behavior and the characteristic time scale for the largest heterogeneity discussed above. A second functional form mentioned by Cortis et al. (2004) is the modified exponential model, which only requires one input parameter.

Another form described in the literature for $\psi(u)$ is the so-called asymptotic model (Cortis and Berkowitz, 2004; Cortis et al., 2004; Margolin and Berkowitz, 2000, 2002, 2004)

$$\psi(u) = \left(1 + au + bu^{\beta_t}\right)^{-1} \quad 0 < \beta_t < 2 \tag{38}$$

where a and b are two additional parameters. It corresponds to the algebraic-in-time PDF model for waiting times. Cortis and Berkowitz (2005) noted that not all combinations of values for β_t, a and b are acceptable. A noticeable case is $0 < \beta_t < 1$, $a = 0$ and $b = 1$. It can be shown that a fractional-in-time advection−dispersion equation can be obtained for that combination of parameters (Berkowitz et al., 2002; Cortis and Berkowitz, 2005; Metzler and Klafter, 2000). In the one-dimensional case, it reads

$$\frac{\partial^{\beta_t} C}{\partial t^{\beta_t}} = -v_\beta \frac{\partial C}{\partial x} + \mathscr{D}_t \frac{\partial^2 C}{\partial x^2} \tag{39}$$

where v_β is a generalized velocity expressed in $[\text{m/s}^{\beta_t}]$ and $\mathscr{D}_\ell$ is expressed in $[\text{m}^2/\text{s}^{\beta_t}]$. Introduction to fractional differential calculus can be found in textbooks (Kilbas et al., 2006; Miller and Ross, 1993; Samko et al., 1993) and e.g. in (Benson, 1998; Benson et al., 2000a; Cushman and Ginn, 2000; Schumer et al., 2001) and references therein. An easy way to understand how fractional derivatives work is to extend the action of Fourier-transforms on integer derivatives to rational order (Benson et al., 2000b)

$$\mathscr{F}\left(\frac{\mathrm{d}^\beta}{\mathrm{d}r^\beta} f(r)\right) = (is)^\beta \mathscr{F}(f(r)) \tag{40}$$

where r is a spatial or temporal coordinate, s is a Fourier-coordinate and β is a rational number. By inverse-transforming this equation, we can find one-dimensional expressions for fractional derivatives. The main feature of these fractional derivatives is that, unlike integer derivatives, they are non-local operators and incorporate an integral from $-\infty$ to r (Benson et al., 2000b). This can be interpreted as a memory-effect (or as a correlation in time or in space of particle displacement).

We now consider spatial anomalous transport, with $\beta_t \geqslant 2$ and $0 < \beta_x < 2$. Benson (1998) and Benson et al. (2000a) showed that describing the dispersive flux of solute particles as proportional to a spatial fractional derivative allows the magnitude of particle velocities (or the size of particle jumps) to be unconstrained. This is an extension of Fick's second law, where the variation of concentration in time can be modeled using a fractional spatial derivative

$$\frac{\partial C}{\partial t} = \mathscr{D}_x \frac{\partial^{\beta_x} C}{\partial x^{\beta_x}} \tag{41}$$

where β_x is the parameter of the Lévy probability density function and $\mathscr{D}_x$ is a fractional longitudinal dispersion coefficient, expressed in $[\mathrm{m}^{\beta_x}/\mathrm{s}]$. If (41) is incorporated in the mass balance, we obtain a fractional-in-space advection-dispersion equation, which can be expressed in the one-dimensional case as (Benson et al., 2000b)

$$\frac{\partial C}{\partial t} = -v\frac{\partial C}{\partial x} + \left(\frac{1+\gamma_B}{2}\right)\mathscr{D}_x \frac{\partial^{\beta_x} C}{\partial x^{\beta_x}} + \left(\frac{1-\gamma_B}{2}\right)\mathscr{D}_x \frac{\partial^{\beta_x} C}{\partial(-x)^{\beta_x}} \tag{42}$$

where γ_B is a skewness coefficient allowing forward jump PDF to be different from backward jump PDF. A complete derivation of this equation as well as useful analytical solutions are provided by Benson (1998) and Benson et al. (2000b). It can be easily checked that taking $\beta_x = 2$ yields (3). As soil heterogeneity is captured by the parameter β_x, $\mathscr{D}_x$ may remain constant and does not need to be scale-dependent anymore. In the multidimensional case, a multi-scaling fractional operator was introduced to encompass different scaling rates of dispersion in different directions (Meerschaert et al., 1999; Meerschaert et al., 2001; Schumer et al., 2003b). In that case, β_x is no longer a scalar but a tensor whose principal directions may not be aligned with the principal directions of the flow field and whose eigenvalues may not be equal in all directions.

Other fractional-order equations are also proposed in the literature. Baeumer et al. (2001) proposed an equation similar to (42) without skewness but with an advection term described using a space-fractional derivative of order $\beta_x/2$. Equations with fractional temporal derivatives of an order up to 2 have also been proposed (Baeumer et al., 2005; Benson et al., 2004; Schumer et al., 2003b), as well as equations involving both time- and space-fractional derivatives (Baeumer et al., 2005; Meerschaert et al., 2002; Metzler and Klafter, 2000).

Dual-domain models

Early in the study of solute transport in porous media, it was realized that a fraction of the fluid present in the pore space of a medium could remain immobile (Coats and Smith, 1964; van Genuchten and Wierenga, 1976). These immobile zones could be either dead-end pores in a porous medium, the rock matrix in a saturated fractured media or clay lenses. Three different approaches can be adopted to account for the influence of these immobile zones. First, an assumption of local equilibrium can be invoked. It supposes that transfer processes occur instantaneously. The second approach uses diffusion to quantify exchange between mobile and immobile zones. The third approach assumes first-order rate-limited exchange, using models borrowed from non-

equilibrium chemical theories. In this section, we only focus on rate-limited and diffusion models. Local equilibrium is an asymptotic case of rate-limited transfer. More elaborate models, accounting for two and more subdivisions of the flow system and considering advection or not in each of the subdivision were also developed (Gerke and van Genuchten, 1993; Jarvis et al., 1991) but are not reviewed here. A detailed comparison of such models is provided by Simunek et al. (2003).

In the case of a two-region model, solutes are divided into a mobile and an immobile region in soils. Solutes present in the mobile zone undergo advection, diffusion and dispersion, while solutes present in the immobile zone only undergo diffusion (i.e. flow velocity in the immobile zone is assumed to be negligible compared to that in the mobile zone). We define C_m and C_{im} the concentrations in the mobile and the immobile phase, respectively. The ADE, as it includes advection and dispersion, is used to describe C_m. It must be however augmented by a term expressing mass exchange with the stagnant zone. In the one-dimensional case, it reads (Carrera et al., 1998; Coats and Smith, 1964; Haggerty and Gorelick, 1995; Schumer et al., 2003a)

$$\frac{\partial C_m}{\partial t} + v\frac{\partial C_{im}}{\partial t} = -v_m\frac{\partial C_m}{\partial x} + D_{L,m}\frac{\partial^2 C_m}{\partial x^2} \tag{43}$$

where $v = \theta_{im}/\theta_m$ is the capacity ratio, θ_m and θ_{im} being the volumetric fractions of mobile and immobile zones, respectively. v_m and $D_{L,m}$ are the velocity and the longitudinal dispersion coefficients in the mobile zone. As an additional unknown appears in (43), an additional relationship is required to solve the problem. If the geometry of the immobile zone is known, a one-dimensional diffusion model can be defined. For example, van Genuchten et al. (1984) studied solute transport in a single cylindrical macropore embedded in a low-porosity rock matrix, and compute C_{im} according to

$$C_{im}(z,t) = \frac{2}{b^2 - a^2}\int_a^b rC_a(z,r,t)\mathrm{d}r \tag{44}$$

where z is aligned in the direction of the macropore and r is the radial distance from the center of the macropore. a is the radius of the macropore and b is the radius of the immobile domain surrounding the cylindrical macropore. C_a is the local concentration in the immobile domain. Solute diffusion in this part of the medium is described using a cylindrical diffusion equation (van Genuchten et al., 1984)

$$\frac{\partial C_a}{\partial t} = \frac{D^d}{r}\frac{\partial}{\partial r}\left(r\frac{\partial C_a}{\partial r}\right) \tag{45}$$

where D^d is an effective diffusion coefficient. van Genuchten et al. (1984) solved (43) using (44) and (45). Other authors have solved similar systems for different geometries of the mobile/immobile system (Brusseau, 1991; Carrera et al., 1998; Haggerty and Gorelick, 1995; Hantush and Marino, 1998a,b; Parker and Valocchi, 1986; Rao et al., 1980).

On a technical level, a more convenient way to handle mobile–immobile domain interactions comes from the assumption of linear non-equilibrium mass transfer (Brusseau, 1991; Coats and Smith, 1964; Haggerty and Gorelick,

1995; Schumer et al., 2003a; van Genuchten and Wagenet, 1989)

$$\frac{\partial C_{\mathrm{im}}}{\partial t} = \omega(C_{\mathrm{m}} - C_{\mathrm{im}}) \tag{46}$$

where ω is a first-order rate coefficient. An exhaustive set of analytical solutions of the system (43) and (46) is given by Toride et al. (1995). The non-dimensional number $Da = \omega L/\theta_{\mathrm{m}} v_{\mathrm{m}}$ is the Damköhler number. It relates the rate of exchange between mobile and immobile phases to advective velocity in the mobile phase. Defining the characteristic times $\tau_\omega = 1/\omega$ and $\tau_{\mathrm{v}} = L/\theta_{\mathrm{m}} v_{\mathrm{m}}$, where L is a characteristic length for advective transport, we have $Da = \tau_{\mathrm{v}}/\tau_\omega$. The latter expresses that the Damköhler number is the ratio of an advective characteristic time scale to a characteristic time scale for exchange with the immobile zone. For low Da, $\tau_{\mathrm{v}} \ll \tau_\omega$, exchange has no time to occur and transport behaves as if there were no immobile phase. For high Da, $\tau_{\mathrm{v}} \gg \tau_\omega$, concentrations in mobile and immobile phases have time to reach local equilibrium and transport can be characterized using an appropriate retardation factor (Bahr and Rubin, 1987; Haggerty and Gorelick, 1995; Parker and Valocchi, 1986; Valocchi, 1985).

The key issue is to estimate the exchange rate ω. Approximate apparent exchange rate coefficients can be derived by comparison with diffusion models. ω is then generally found to be proportional to $\omega \sim D^d/A^2$, A being a characteristic lens size (Carrera et al., 1998; Haggerty and Gorelick, 1995; Zhang et al., 2007a). Other upscaling methods, such as homogenization (Auriault and Lewandowska, 1995; Panfilov, 2000) or volume-averaging (Cherblanc et al., 2003, 2006; Golfier et al., 2007; Moyne, 1996; Quintard et al., 2001) allow keeping the coupling between micro-scale physics and macroscale parameters through some closure problems. The upscaling of exchange rate coefficients and diffusion coefficients are however separate problems, beyond the scope of this review. The reader is referred to the review by Cushman et al. (2002) for more details.

Although experimental results show an equivalence between diffusion models and single-rate mass transfer models under simple flow and transport conditions (Nkedi-Kizza et al., 1984), some authors are relatively mitigated regarding the general applicability of single-rate models (Bajracharya and Barry, 1997; Griffioen, 1998; Griffioen et al., 1998). First, the single-rate model is not able to exactly reproduce matrix diffusion (Carrera et al., 1998; Dentz and Berkowitz, 2003; Haggerty and Gorelick, 1995). Then, results from solute transport conducted are various scales reveal that exchange rates are found to be scale-dependent (Haggerty et al., 2004). This phenomena is typically explained (1) by the presence of multiple timescales of mass transfer (Haggerty and Gorelick, 1995; Haggerty et al., 2004), (2) by slow advection (Guswa and Freyberg, 2000; Haggerty et al., 2004; Zinn et al., 2004), which results in concentration distributions having similar shapes as if they were resulting from a mobile–immobile domain interaction, and (3) by nonlinear hysteretic sorption (Haggerty et al., 2004; Jaekel et al., 1996). It is also worth mentioning that stochastic extensions, similar to those reported in this paper for the ADE, have been developed for the single-rate MIM (Huang and Hu, 2000; Huang et al., 2003).

Haggerty and Gorelick (1995) extended the single-rate model to a multirate solute transport equation

$$\frac{\partial C_{\mathrm{m}}}{\partial t} + \sum_{i=1}^{N} v_i \frac{\partial(C_{im})_i}{\partial t} = -v_{\mathrm{m}} \frac{\partial C_{\mathrm{m}}}{\partial x} + D_{L,m} \frac{\partial^2 C_{\mathrm{m}}}{\partial x^2} \tag{47}$$

with N additional equations

$$\frac{\partial (C_{im})_i}{\partial t} = \omega_i \big(C_{\mathrm{m}} - (C_{im})_i \big) \quad i = 1, \ldots, N \tag{48}$$

In this case, $v_i = (\theta_{\mathrm{im}})_i / \theta_{\mathrm{m}}$ includes the volumetric proportion of immobile zone i. In case ω_i are continuously distributed, the sum in (47) must be replaced by an integral (Dentz and Berkowitz, 2003; Haggerty et al., 2000; Wang et al., 2005). Haggerty and Gorelick (1995) demonstrated the equivalence between diffusion and multirate models by deriving a series solutions for ω_i and v_i that could match diffusion models.

In the case of single-rate exchange, (46) can also be expressed as (Schumer et al., 2003a)

$$\frac{\partial C_{\mathrm{im}}}{\partial t} = f(t) * C_{\mathrm{m}} + f(t)(C_{\mathrm{m}}(x,0) - C_{\mathrm{im}}(x,0)) \tag{49}$$

where $f(t) = \omega e^{-\omega t}$ is a memory function and $*$ denotes convolution. Haggerty et al. (2000) showed that the memory function can take many forms, considering various diffusion models or multirate exchange with various exchange rate distributions. In the latter case, $f(t)$ is a sum of exponential functions, each corresponding to a single rate. Haggerty et al. (2000) used the properties of the memory function to discern between single rate and multirate transport by considering the late-time behavior of breakthrough curves. For single-rate exchange between mobile and immobile zones, late-time behavior is governed by a single exponential in time, and the plot of $\log(C)$ versus time should be linear for $t \gg \langle t \rangle$. In the case of multirate mass transport, late-time behavior is governed by a sum of exponentials, that are actually equivalent to an algebraic (power-law) tail. Therefore, the plot of $\log(C)$ versus $\log(t)$ should be linear for $t \gg \langle t \rangle$.

Application to the reference example

Third- or fourth-order PDE's usually do not represent a valuable alternative to the classical advection–dispersion equation, mainly due to the difficulty to derive analytical or numerical solutions. We therefore focus here on telegraph equations, CTRW and fractional-order equations, and mobile–immobile models. The main issue with upscaled transport equations lies in the estimation of their parameters: there are currently few methods available to link them with the spatial structure of the subsurface. Curve-fitting is then required to estimate parameter values from observed concentration distributions. In this section, we compare upscaled transport equations with the aid of the cumulative mass arrival function $Q(t,x)$, or cumulative breakthrough curve (BTC), at an arbitrary control plane at location x. $Q(t,x)$ is computed as the relative number of particles that have already crossed the control plane at time t. We use here three reference curves, observed at control planes located 25λ, 50λ and 75λ downstream of the injection zone, respectively (Fig. 1c).

The effective relaxation time τ_e in Scheidegger telegraph equation (32) can be estimated from the apparent longitudinal dispersivity, which converges according to a single exponential function with time (Berentsen, 2003)

$$\alpha_L^*(t) = \alpha_L^*(\infty)\left(1 - \exp\left(-\frac{t}{\tau_e}\right)\right) \qquad (50)$$

In the case of a perfectly stratified aquifer, Berentsen (2003) showed that $\alpha_L^*(\infty) = \sigma_v^2 \tau_e / \langle v_1 \rangle$, σ_v^2 being the variance of the velocity profile. We assumed that this result also holds for three-dimensional situations in order to apply Berentsen's method. The variance of the velocity field is $\sigma_v^2 = 0.202$ m^2/d^2 and $\sigma_v^2 = 10.89$ m^2/d^2 for case $\sigma_Y^2 = 2$ and $\sigma_Y^2 = 8$, respectively. Fitting of (50) onto the time histories of apparent dispersivity (shown in Figs. 5 and 6) yields $\tau_e = 16.80$ days and $\tau_e = 3.93$ days for case $\sigma_Y^2 = 2$ and $\sigma_Y^2 = 8$, respectively. Since the goal of using upscaled transport equations is to characterize transport using scale-invariant parameters, we also compare the results to BTC's computed from the ADE with local (microscopic) dispersivity values (Fig. 7). This illustrates the level of error resulting from the use of the ADE using transport parameters measured at a small scale (e.g. using column laboratory tests). Scaling the longitudinal dispersivity according to (50) and using the ADE do not yield BTC's significantly different from the solution of Scheidegger telegraph equation. This is a result of the Gaussian shape of the breakthrough curves and highlights that the ADE combined with upscaling methods

for dispersivity could also have been used to model concentration distributions. In the high variance case, results are of a lower quality, but exhibit similar trends. The practical improvement of using Scheidegger telegraph equation seems therefore relatively limited and only resides in the reassuring use of scale-invariant parameters, as well as maybe a better modeling of concentration distributions at early times. The observed discrepancy between observed BTC's and theoretical models at larger distance probably comes from an underestimation of the constant asymptotic longitudinal dispersivity. Indeed, τ_e is determined based on early-time data ($t < 486$ days and $t < 86$ days, respectively for the low-variance and the high-variance case). As expected, anomalous transport is more pronounced for case $\sigma_Y^2 = 8$, since the BTC's exhibit slow late-time convergence to 1. This effect cannot be correctly modeled by Scheidegger telegraph equation.

The Matlab CTRW toolbox (Cortis and Berkowitz, 2005) is used to characterize BTC's using temporally anomalous transport models. The truncated power law model (37) is used for the waiting time PDF. Two sets of fits are performed. First, each of the three reference BTC is individually analyzed. A nearly perfect fit can be reached in most situations (Fig. 8) but all parameters are found to be scale-dependent (Table 3). For the case $\sigma_Y^2 = 2$, β_t is close or equal to 2, indicating that observed BTC's have a Gaussian shape, with few early arrivals and a rapid convergence. This is consistent with the study by Trefry et al. (2003),
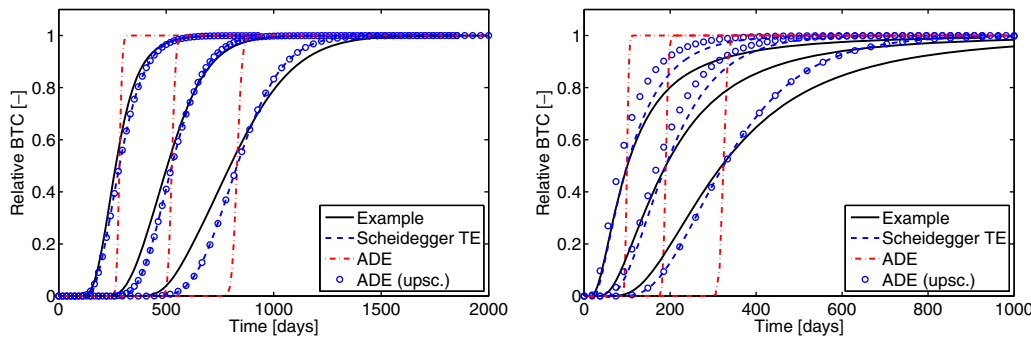
Figure 7 Comparison of cumulative breakthrough curves with Scheidegger telegraph equation and with the classical ADE (with and without scaling the longitudinal dispersivity). Theoretical curves are centered on observed data to avoid any additional shift caused by a misprediction of mean velocities. Case $\sigma_Y^2 = 2$ (left), and case $\sigma_Y^2 = 8$ (right).
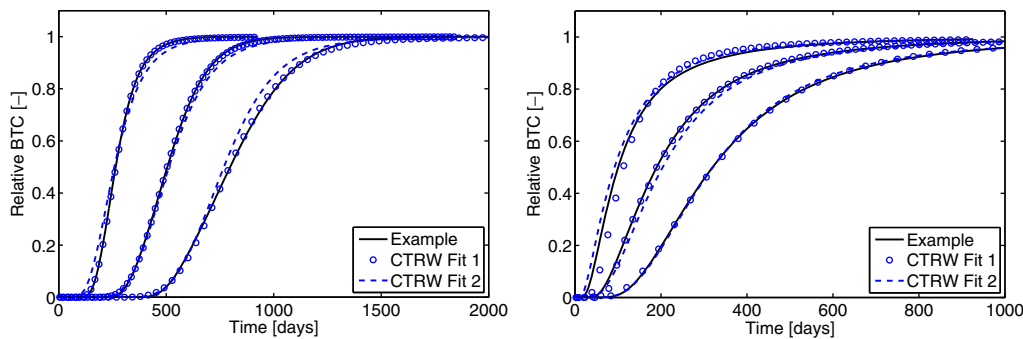
Figure 8 Comparison of cumulative breakthrough curves with temporally anomalous models. Individual (Fit 1) and simultaneous (Fit 2) analysis of BTC's. Case $\sigma_Y^2 = 2$ (left), and case $\sigma_Y^2 = 8$ (right).

Table 3 Fitted transport parameters for temporally and spatially anomalous models

	$\sigma_Y^2 = 2$				$\sigma_Y^2 = 8$			
	Individual fits				Individual fits			
	BTC1	BTC2	BTC3	Global fit	BTC1	BTC2	BTC3	Global fit
Temb. anom.								
β_t (−)	2.00	2.00	1.84	1.84	1.38	1.60	1.51	1.54
v (m/d)	0.48	0.50	0.54	0.57	2.09	1.63	1.80	1.69
α_L (m)	3.86	8.19	9.98	7.95	6.32	24.3	31.8	23.2
t_1 (d)	2.65	1.58	2.13	1.98	3.03	10.9	5.35	8.61
Spat. anom.								
β_x (−)				1.51				1.26
v (m/d)	0.49	0.50	0.47	0.48	1.38	1.38	1.20	1.32
$\mathscr{D}_x$ (m^{β_x}/d)	0.76	0.90	1.01	0.89	4.64	4.68	3.77	4.36
γ_B (−)	−0.55	−0.44	−0.44	−0.48	−0.00	−0.01	−0.03	−0.01

conducted on two-dimensional lognormal permeability fields with $\sigma_Y^2 < 4$: they used the fractional-in-time ADE (39) and found β_t values close to 1, indicating that concentration distributions do not clearly exhibit a temporally anomalous behavior. The overall quality of the fit is similar to what could be obtained using the ADE and an upscaled dispersivity value (see e.g. Fig. 7). For the case $\sigma_Y^2 = 8$, β_t is much lower than 2. If the parameters are still scale-dependent, a significant improvement is observed in the modeling of the tails of the BTC's. This definitely suggests that anomalous transport models are particularly suited to model transport in highly heterogeneous three-dimensional aquifers. Then, a single set of parameters is determined by simultaneously analyzing the three reference BTC's. We find $\beta_t = 1.84$ and $\alpha_L = 7.95$ m for case $\sigma_Y^2 = 2$, and $\beta_t = 1.54$ and $\alpha_L = 23.2$ m for case $\sigma_Y^2 = 8$. Although this approach does not allow parameters to be scale-dependent, it appears that resulting fits are still in a good agreement with the numerical results. t_2 in (37) was always found always larger than 10^5 days.

We turn now to spatially anomalous transport models. β_x is estimated based on the slope of α_L^* versus measurement scale plotted on a log–log scaled graph (Benson, 1998). We obtain here $\beta_x = 1.51$ and $\beta_x = 1.26$ for case $\sigma_Y^2 = 2$ and case $\sigma_Y^2 = 8$, respectively. $\mathscr{D}_x$ and γ_B are estimated by fitting the solution of (42) onto early-time concentration data (corresponding to relative concentrations below

84%). If the value of β_x allows the modeling of the scale effect in apparent dispersivity, its value however yields heavy-tailed concentrations distributions, which does not match numerical results in both cases (Fig. 9). It appears that $\mathscr{D}_x$ and γ_B are relatively scale-invariant (Table 3), and taking a unique set of parameter (Fit 2 − computed as the mean of each parameter) does not yield a significant difference.

Finally, the single-rate mobile–immobile model is illustrated with the aid of the reference example. For spherical inclusions, an approximate exchange rate is given by $\omega \approx \pi^2 D^d / A^2 = 1.92 \ 10^{-5}$ days^{-1} (accounting for $A = 4\lambda/3$, λ being the correlation length characterizing the log-permeability field) (Haggerty and Gorelick, 1995). θ_m can be estimated by comparing the apparent velocity for each BTC with the mean Darcy velocity v_D of the aquifer. We obtain $\theta_m = 0.28$, $\theta_m = 0.27$ and $\theta_m = 0.29$ for BTC1, BTC2 and BTC3, respectively, for case $\sigma_Y^2 = 2$. For case $\sigma_Y^2 = 8$, we have $\theta_m = 0.29$, $\theta_m = 0.27$ and $\theta_m = 0.30$ for BTC1, BTC2 and BTC3, respectively. The average values for the capacity ratio are therefore $v = 0.43$ and $v = 0.40$ for the low- and high-variance case. Using the local dispersivity with this set of parameters does however not yield a good agreement with observed BTC's (Fit 1, Fig. 10). The only improvement with respect to the ADE is the modeling of the discrepancy between observed mean velocities and v_D / θ. The use of an upscaled longitudinal dispersivity (obtained, e.g. from the
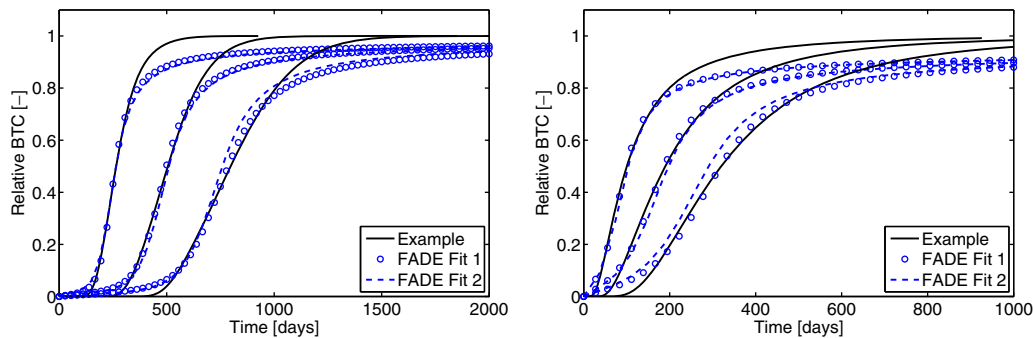
Figure 9 Comparison of cumulative breakthrough curves with spatially anomalous models. Individual (Fit 1) and simultaneous (Fit 2) analysis of BTC's. Case $\sigma_Y^2 = 2$ (left), and case $\sigma_Y^2 = 8$ (right).
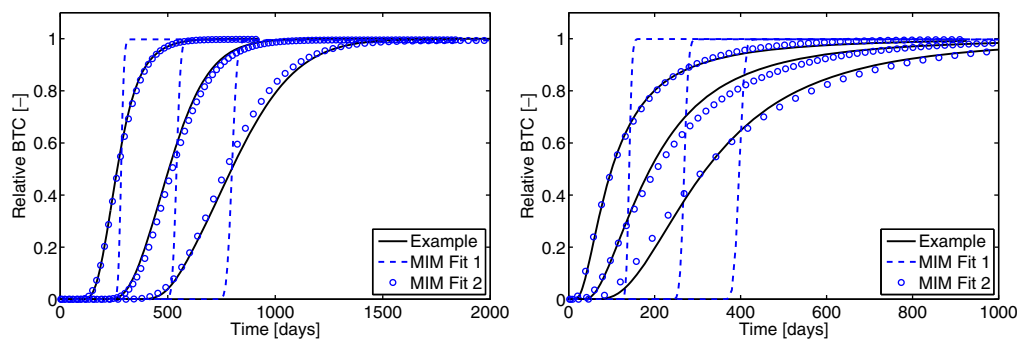
Figure 10   Comparison of cumulative breakthrough curves with a single-rate mobile—immobile model. A priori prediction without (Fit 1) and with (Fit 2) an upscaled longitudinal dispersivity. Case $\sigma_Y^2 = 2$ (left), and case $\sigma_Y^2 = 8$ (right).

classical stochastic theory) however allows a satisfactory matching of the three BTC's (Fit 2, Fig. 10). Moreover, in the high variance case, the long tails of the BTC's are reasonably predicted. Although we do not provide multirate mass exchange models of the reference example under investigation here, it is expected that these models would significantly improve the observed limitations of the single-rate first-order approach.

It appears that the quality of the results obtained here is less homogeneous than when applying upscaling methods for dispersivity. If reasonable fits of concentration distributions could be obtained using Scheidegger telegraph equation and temporal CTRW, the quality of the spatial CTRW model was lower. MIM could not be applied using scale-invariant transport parameters and therefore appear to be of a more limited use in our particular reference examples. However, the combined use of a single-rate MIM with upscaled values of longitudinal dispersivity allowed a good match of observed concentration distributions, reconciling the difference between mean aquifer velocity and mean plume velocity. We can conclude therefrom that transport mainly occurs in high- or medium-permeability zones of the reference aquifer model, with very little interaction with low-permeability zones, and that heterogeneity in the mobile zone causes an increased longitudinal spreading of the solute plume.

Further insights into upscaled transport models

In this section, only a small portion of the full literature on upscaled equations for solute transport in the subsurface was presented. For example, Cushman et al. (1994) and Neuman (1993) have developed very general approaches, of which several specific fractional advection—dispersion equations are found to be particular cases (Zhang et al., 2007a). We refer to the reviews by Cushman and Hu (1995) and Cushman et al. (2002) for more details on these other approaches. Similarly, we only briefly evoked volume-averaging approaches and homogenization theory in this work, and refer the reader to the reviews of Cushman et al. (2002) and Berkowitz et al. (2006), and the book of Whitaker (1999).

Replacing the classical advection—dispersion equation by a telegraph equation was suggested a relatively long time ago (Scheidegger, 1960). The fundamental issues underlying the application of (32) to field situations are that (1) diffu-

sion is neglected, and (2) velocity distributions cannot be skewed. This basically limits the applicability of this equation to situations in which the advection—dispersion equation could be used with an upscaled dispersion coefficient. Although there is an increase in the complexity of the solution of (32) with respect to the ADE, the approach is more elegant since the scale effect is intrinsically built-in.

The development and application of CTRW and fractional ADE's is currently a very active and evolving research area, and these models are being applied to problem as varied as transport of solutes in fractured media (Reeves et al., 2008), transport of colloids (Cortis et al., 2006), or even transport of emulsions in porous media (Cortis and Ghezzehei, 2007). However, a widespread use of these non-Fickian models and the progressive abandonment of the ADE will require a drastic change in practitioners habits. This change is not likely to happen as long as efficient numerical tools adapted to field situations are not developed. The current version of the CTRW toolbox allows for the modeling of one- and two-dimensional problems in homogeneous domain, but plans for extension to heterogeneous fields exist (Cortis and Berkowitz, 2005). Fractional ADE's are currently receiving more attention, since three-dimensional numerical codes adapted to solve field problems are being developed (Zhang et al., 2008). In field situations, it is also likely that chemical processes will take place, and sorption and chemical reactions have to be implemented in these codes.

As for the stochastic upscaling methods of dispersivity, some of the models presented here are adapted to situations where dispersion coefficients converge to constant values, while other are preferably used in pre-ergodic situations. Scheidegger telegraph equation and the CTRW model with the truncated power law kernel function both predict convergence to a constant asymptotic macrodispersivity. Scheidegger telegraph equation includes a parameterization very similar to that of the upscaling methods for longitudinal dispersivity. The relaxation time τ_e could be easily converted into a characteristic length using some measure of the average velocity, while σ_v^2 is an explicit description of the variability of the velocity field. Similarly, the CTRW model with a truncated power law kernel uses a characteristic time to describe the transition to an asymptotic constant apparent dispersion coefficient. On the contrary, the space-fractional ADE typically predicts a constant linear increase in apparent dispersion coefficients,

similarly to the fractal extension of the stochastic theory. There are actually underlying connections between the fractal dimension of a heterogeneous medium, and the order of the fractional Laplacian in (42). We refer to Kolwankar and Gangal (1996), who elaborate on the explicit connections between self-similar fractals and the fractional derivative.

Summary and conclusion

In this paper, we focused on inert solute transport in saturated heterogeneous media. Although we only focused on longitudinal transport, two- or three-dimensional analytical expressions are usually also reported in the literature for the models presented.

A set of stochastic upscaling methods for longitudinal dispersivity are first reviewed. Although differing from each other, all these methods require a characterization of the heterogeneity in terms of (1) an average permeability contrast (i.e. a variance) and (2) a characteristic length scale (finite or infinite). The average perturbation of the velocity field resulting from heterogeneity is calculated and converted into a macroscale dispersion coefficient. Potential alternatives to the ADE are also reviewed. Higher-order partial differential equations are not found to be valuable options due to their increased complexity, but telegraph equations could be more appropriate. CTRW and fractional-order partial differential equations have been recently brought to the field of hydrogeology and, although requiring a relatively unusual mathematical formalism, they can also be more appropriate to model solute transport. MIM are found to be a third class of transport equations that can account for non-Fickian effects in dispersive processes.

We illustrated the application of the models using two large three-dimensional numerical examples, solved using MODFLOW 2000 and a particle-tracking software. We used a single realization of a spatially correlated permeability field, of which we varied the variance from $\sigma_Y^2 = 2$ to $\sigma_Y^2 = 8$. Solute was released over a rather limited portion of the synthetic aquifer, and traveled over a limited distance. The main implication for the application of upscaling methods is that the plume only sampled a very limited portion of the aquifer and did not experience the full variability of the velocity field. Although these conditions are rather non-ideal for the application of semi-analytical results as presented in this paper, they are not unusual for a field situation. We emphasize that due to these limitations, the results reported here are mainly aimed at providing a relatively qualitative framework for the comparison of the methods and models, and their respective performances must be seen as situation-dependent. A more rigorous study would require some Monte Carlo analysis to address the problem of limited ergodic conditions, and other models for the structure of the permeability field should be considered.

Analysis of the spatial moments of the solute plume showed that apparent longitudinal dispersivity converged to a value about 100 times larger than the local dispersivity when $\sigma_Y^2 = 2$, and to about 400 times the local value when $\sigma_Y^2 = 8$. Upscaling methods for longitudinal dispersivity all

allowed the prediction of the observed scale-effect within a correct order of magnitude for the low-variance case. As field variograms can be scattered, the results that we obtained tend to show that a correct order of magnitude should be reached in the prediction of asymptotic longitudinal dispersivity by all analyzed models, as long as the main trends in correlation are accounted for. In the high-variance case, upscaling methods for longitudinal dispersivity yielded less uniform results. Inclusion methods turned out to produce close estimates of macrodispersivity. Provided that an appropriate flow factor is adopted, classical stochastic methods also yielded a reasonable prediction of α_L^*. However, fractal methods did not provide satisfactory results.

We also compared cumulative breakthrough curves evaluated at three reference control planes. In the low-variance case, they were all found to have a Gaussian shape, with few early arrivals and short late-time tails. Therefore, only Scheidegger telegraph equation and temporal CTRW with $\beta_t > 2$ could allow the correct prediction of the apparent spreading of concentration distributions without relying on an upscaled dispersivity. The application of temporal CTRW required a dispersivity about 40 times larger than the local value and the space-FADE managed to predict apparent dispersivity at the expense of largely overestimated tails. The single-rate MIM also required an upscaled longitudinal dispersivity but could reconcile the discrepancy between the apparent plume velocity and the overall mean velocity of the aquifer. In the high-variance case, we observed non-Gaussian breakthrough curves, as a result of the velocity distribution in the aquifer. In this particular case, temporal CTRW were found to be the best models, although lower constraints were imposed on their parameters. Spatially anomalous models overestimated the tail of the BTC's, but we did not allow the main parameter β_x to vary. We emphasize that spatially anomalous transport models have been successfully applied to other situations of solute transport in heterogeneous aquifers (Benson et al., 2000b; Benson et al., 2001). Multiple-rate mass exchange models were not specifically investigated within the scope of the reference example. They are believed to yield modeling results comparable to those obtained with the time-CTRW model, since they are mathematically equivalent.

There are fundamental differences between the different upscaling strategies reviewed in this paper. Some are based on structural properties which are observable (at least in principle) while other need to be fitted to concentration data, having mainly descriptive power. Stochastic upscaling methods for longitudinal dispersivity are relatively commonly used, because the link between heterogeneity and solute dispersion is explicitly accounted for. Moreover, geostatistical methods have been used in the field for several decades, and the characterization of aquifers in terms of variance and correlation length is usually well mastered by practitioners. On the contrary, upscaled transport models require an extended parametrization of the transport problem that is not directly related to the cause of the scale effect (i.e. heterogeneity). What is missing is precisely the link between both approaches: further research efforts are needed in order to establish the link between upscaling methods and upscaled transport equations. As long as effective and reliable field methods are not developed for the

characterization of upscaled models, it is unlikely that they become widely used. In this framework, MIM's and in particular multiple-rate MIM's, are believed to be one of the most promising upscaled models. It directly builds upon the classical ADE and can integrate any level of complexity by augmenting the number of exchange terms. MIM's can be combined with upscaling methods for dispersivity while modeling anomalous transport resulting from diffusive mass exchanges. With a proper parametrization of the velocity and the mobile porosity, the presence of highly permeable connected pathways can be accounted for as well.

Finally, if we applied each model to the reference examples in a rather systematic fashion, such an approach is not a viable option for the practitioner. The choice of an appropriate model is typically case-dependent and should be made by considering at least three important pieces of information:

- First, as appearing from the reference examples, the level of heterogeneity must play a role in the choice of a conceptual transport model. In situations with a relatively low level of heterogeneity, one should be tempted to use stochastic theories and compute upscaled values of dispersivity to be substituted in the advection—dispersion equation. Solving the ADE with time- or space-dependent dispersion coefficients, either numerically (Pickens and Grisak, 1981) or analytically (Aral and Liao, 1996; Huang et al., 1996; Hunt, 1998; Hunt, 2002; Logan, 1996; Pang and Hunt, 2001; Yates, 1990; Zou et al., 1996) is another option. The third possibility is to use Scheidegger telegraph equation. Although its mathematical formalism is slightly more elaborate than the ADE, it intrinsically embodies the scale effect in apparent dispersivity. When permeability contrasts are higher (e.g. $\sigma_Y^2 > 4$), mobile—immobile models and CTRW should be preferred, since they are able to handle diffusive transport when it cannot be neglected compared to advective transport.
- Then, the scale at which predictions have to be made, compared to the characteristic length of heterogeneity will also play a role in the choice of an adequate method. If predictions have to be made at a small scale, anomalous transport models should usually be preferred, because concentration distributions are not likely to be Gaussian. A fractal method could also be used to compute apparent dispersion coefficients. If predictions are made at a large scale and ergodic conditions are likely to be met, models relying on the asymptotic long distance limit, such as the classical stochastic method, inclusion models, or Scheidegger telegraph equation, could be used with relative confidence.
- Finally, the type of available data (e.g. permeability, head or concentration) is an important feature of the (inverse) modeling problem. Upscaling methods for longitudinal dispersivity are based on a parametrization of the structure of the subsurface. No a priori information on concentration distribution is needed to scale transport up. On the contrary, upscaled transport equations almost systematically require concentration data at the scale of interest, and model parameters must be obtained by fitting of the corresponding analytical solution onto observed BTC's.

References

Abramowitz, M., Stegun, I., 1970. Handbook of Mathematical Functions. Dover Publications Inc., New York.

Adler, P.M., 1996. Transport in fractal porous media. Journal of Hydrology 187, 197—213.

Aral, M.M., Liao, B., 1996. Analytical solutions for two-dimensional transport equation with time-dependent dispersion coefficients. Journal of Hydrologic Engineering 1 (1), 20—32.

Attinger, S.M., Dentz, M., Kinzelbach, H., Kinzelbach, W., 1999. Temporal behavior of a solute cloud in a chemically heterogeneous porous medium. Journal of Fluid Mechanics 386, 77—104.

Auriault, J.L., Lewandowska, J., 1995. Non-Gaussian diffusion modeling in composite porous media by homogenization. Tail effect. Transport in Porous Media 21 (1), 47—70.

Baeumer, B., Benson, D.A., Meerschaert, M.M., Wheatcraft, S.W., 2001. Subordinated advection—dispersion equation for contaminant transport. Water Resources Research 37 (6), 1543—1550.

Baeumer, B., Benson, D.A., Meerschaert, M.M., 2005. Advection and dispersion in time and in space. Physica A 350, 245—262.

Bahr, J.M., Rubin, J., 1987. Direct comparison of kinetic and local equilibrium formulations for solute transport affected by surface reactions. Water Resources Research 23 (3), 438—452.

Bajracharya, K., Barry, D.A., 1997. Nonequilibrium solute transport parameters and their physical significance: numerical and experimental results. Journal of Contaminant Hydrology 24, 185—204.

Bear, J., 1972. Dynamics of Fluids in Porous Media. American Elsevier Publishing Company.

Bellin, A., Salandin, P., Rinaldo, A., 1992. Simulation of dispersion in heterogeneous porous formations: statistics, first-order theories, convergence of computations. Water Resources Research 28 (9), 2211—2227.

Bellin, A., Pannone, M., Fiori, A., Rinaldo, A., 1996. On transport in porous formations characterized by heterogeneity of evolving scales. Water Resources Research 32 (12), 3485—3496.

Benson, D.A., 1998. The Fractional Advection—Dispersion Equation: Development and Application. University of Nevada, Reno, NV, USA, Ph.D. Thesis.

Benson, D.A., Wheatcraft, S.W., Meerschaert, M.M., 2000a. The fractional-order governing equation of Lévy motion. Water Resources Research 36 (6), 1413—1423.

Benson, D.A., Wheatcraft, S.W., Meerschaert, M.M., 2000b. Application of a fractional advection—dispersion equation. Water Resources Research 36 (6), 1403—1412.

Benson, D.A., Schumer, R., Meerschaert, M.M., Wheatcraft, S.W., 2001. Fractional dispersion, Lévy motion, and the MADE tracer tests. Transport in Porous Media 42, 211—240.

Benson, D.A., Tadjeran, C., Meerschaert, M.M., Farnham, I., Pohll, G., 2004. Radial fractional-order dispersion trough fractured rocks. Water Resources Research 40. doi:10.1029/2004WR003314.

Benson, D.A., Meerschaert, M.M., Baeumer, B., Scheffler, H.-P., 2006. Aquifer operator-scaling and the effect on solute mixing and dispersion. Water Resources Research 43. doi:10.1029/2004WR003755.

Berentsen, C., 2003. Upscaling of flow in porous media from a tracer perspective. Ph.D. thesis, T.U. Delft, The Netherlands.

Berentsen, C.W.J., Verlaan, M.L., van Kruijsdijk, C.P.J.W., 2005. Upscaling and reversibility of Taylor dispersion in heterogeneous porous media. Physical Review E 71. doi:10.1103/PhysRevE.71.046308.

Berkowitz, B., Scher, H., 1995. On characterization of anomalous dispersion in porous and fractured media. Water Resources Research 31 (6), 1461–1466.

Berkowitz, B., Kosakowski, G., Margolin, G., Scher, H., 2001. Application of continuous time random walk theory to tracer test measurements in fractured and heterogeneous porous media. Groundwater 39 (4), 593–604.

Berkowitz, B., Klafter, J., Metzler, R., Scher, H., 2002. Physical pictures of transport in heterogeneous media: advection–dispersion, random walk and fractional derivatives formulations. Water Resources Research 38 (10).

Berkowitz, B., Cortis, A., Dentz, M., Scher, H., 2006. Modeling non-Fickian transport in geological formations as a continuous time random walk. Reviews of Geophysics 44. doi:10.1029/2005RG000178.

Brusseau, M.L., 1991. Application of a multiprocess nonequilibrium sorption model to solute transport in a stratified porous medium. Water Resources Research 27 (4), 589–595.

Camacho, J., 1993a. Thermodynamics of Taylor dispersion: constitutive equations. Physical Review E 47 (2), 1049–1053.

Camacho, J., 1993b. Purely global model for Taylor dispersion. Physical Review E 48 (1), 310–321.

Camacho, J., 1993c. Thermodynamic functions for Taylor dispersion. Physical Review E 48 (3), 1844–1849.

Carle, S.F., Fogg, G.E., 1996. Transition probability-based indicator geostatistics. Mathematical Geology 28 (4), 453–476.

Carle, S.F., Fogg, G.E., 1997. Modeling spatial variability with one- and multidimensional continuous-lag Markov chains. Mathematical Geology 29 (7), 891–918.

Carrera, J., Neuman, S.P., 1986. Estimation of aquifer parameters under transient and steady-state conditions. 1. Maximum likelihood method incorporating prior information. Water Resources Research 22 (2), 199–210.

Carrera, J., Sanchez-Vila, X., Benet, I., Medina, A., Galarza, G., Guimera, J., 1998. On matrix diffusion: formulations, solution methods and qualitative effects. Hydrogeology Journal 6, 178–190.

Chen, J., Hubbard, S.S., Rubin, Y., 2001. Estimating the hydraulic conductivity at the South Oyster site from geophysical tomographic data using Bayesian techniques based on the normal linear regression model. Water Resources Research 37 (6), 1603–1613.

Cherblanc, F., Ahmadi, A., Quintard, M., 2003. Two-medium description of dispersion in heterogeneous porous media: calculation of macroscopic properties. Water Resources Research 39 (6). doi:10.1029/2002WR001559.

Cherblanc, F., Ahmadi, A., Quintard, M., 2006. Two-medium description of dispersion in heterogeneous porous media: comparison between theoretical predictions and numerical experiments. Advances in Water Resources 30 (5), 1127–1143.

Chin, D.A., 1997. An assessment of first-order stochastic dispersion theories in porous media. Journal of Hydrology 199, 53–73.

Cirpka, O.A., Kitanidis, P.K., 2001. Sensitivity of temporal moments calculated by the adjoint-state method and joint inversing of head and tracer data. Advances in Water Resources 24, 89–103.

Coats, K.H., Smith, B.D., 1964. Dead-end pore volume and dispersion in porous media. Society of Petroleum Engineering Journal 4, 73–84.

Cortis, A., Berkowitz, B., 2004. Anomalous transport in classical soil and sand columns. Soil Science Society of America Journal 68, 1539–1548.

Cortis, A., Berkowitz, B., 2005. Computing anomalous contaminant transport in porous media: the CTRW Matlab toolbox. Groundwater 43 (6), 947–950.

Cortis, A., Gallo, C., Scher, H., Berkowitz, B., 2004. Numerical simulation of non-Fickian transport in geological formations with multiple-scale heterogeneities. Water Resources Research 40. doi:10.1029/2003WR002750.

Cortis, A., Harter, T., Hou, L., Atwill, E.R., Packman, A., Green, P., 2006. Long-time elution of Cryptosporidium Parvum Oocysts in porous media. Water Resources Research 42 (12), W12S13.

Cortis, A., Ghezzehei, T.A., 2007. On the transport of emulsions in porous media. Journal of Colloid and Interface Science 313 (1), 1–4.

Cushman, J.H., 1991. On diffusion in fractal porous media. Water Resources Research 27, 643.

Cushman, J.H., Ginn, T.R., 1993. Nonlocal dispersion in media with continuously evolving scales of heterogeneity. Transport in Porous Media 13, 123.

Cushman, J.H., Hu, B.X., Ginn, T.R., 1994. Nonequilibrium statistical mechanics of preasymptotic dispersion. Journal of Statistical Physics 75 (5/6), 859–878.

Cushman, J.H., Hu, B.X., 1995. A resumé of nonlocal transport theories. Stochastic Environmental Research and Risk Assessment 9 (2), 105–116.

Cushman, J.H., Ginn, T.R., 2000. Fractional advection–dispersion equation: a classical mass-balance with convolution-Fickian flux. Water Resources Research 36 (12).

Cushman, J.H., Bennethum, L.S., Hu, B.X., 2002. A primer on upscaling tools for porous media. Advances in Water Resources 25, 1043–1067.

Cvetkovic, V., Haggerty, R., 2002. Transport with multiple-rate exchange in disordered media. Physical Review E 65. doi:10.1103/PhysRevE.65.051308.

Dagan, G., 1979. Models of groundwater flow in statistically homogeneous porous formations. Water Resources Research 15 (1), 47–63.

Dagan, G., 1984. Solute transport in heterogeneous formations. Journal of Fluid Mechanics 145, 151–177.

Dagan, G., 1988. Time-dependent macrodispersion for solute transport in anisotropic heterogeneous aquifer. Water Resources Research 24 (9), 1491–1500.

Dagan, G., 1989. Flow and Transport in Porous Formations. Springer, New-York.

Dagan, G., 1990. Transport in heterogeneous porous formations: spatial moments, ergodicity, and effective dispersion. Water Resources Research 26 (6), 1281–1290.

Dagan, G., Bresler, E., 1979. Solute dispersion in unsaturated heterogeneous soil at the field scale. 1. Theory. Soil Science Society of America Journal 43, 461–467.

Dagan, G., Lessoff, S.C., 2001. Solute transport in heterogeneous formations of bimodal conductivity distribution. 1. Theory. Water Resources Research 37 (3), 465–472.

Dagan, G., Fiori, A., 2003. Time-dependent transport in heterogeneous formations of bimodal structure. 1. The model. Water Resources Research 39 (5). doi:10.1029/2002WR001396.

Dagan, G., Fiori, A., Jankovic, I., 2003. Flow and transport in highly heterogeneous formations. 1. Conceptual framework and validity of first-order approximations. Water Resources Research 39 (9). doi:10.1029/2002WR001717.

de Josselin de Jong, G., 1958. Longitudinal and transverse diffusion in granular deposits. Transactions, American Geophysical Union 39, 67–74.

Dentz, M., Kinzelbach, H., Attinger, S., Kinzelbach, W., 2000a. Temporal behavior of a solute cloud in a heterogeneous porous medium. 1. Point-like injection. Water Resources Research 36 (12), 3591–3604.

Dentz, M., Kinzelbach, H., Attinger, S., Kinzelbach, W., 2000b. Temporal behavior of a solute cloud in a heterogeneous porous medium. 2. Spatially extended injection. Water Resources Research 36 (12), 3605–3614.

Dentz, M., Berkowitz, B., 2003. Transport behavior of a passive solute in continuous time random walks and multirate mass transfer. Water Resources Research 39 (5). doi:10.1029/2001WR001163.

Dentz, M., Cortis, A., Scher, H., Berkowitz, B., 2004. Time behavior of solute transport in heterogeneous media: transition from anomalous to normal transport. Advances in Water Resources 27, 155—173.

Desbarats, A.J., 1990. Macrodispersion in sand-shale sequences. Water Resources Research 26 (1), 153—163.

Di Federico, V., Neuman, S.P., 1998. Transport in multiscale log conductivity fields with truncated power variograms. Water Resources Research 34 (5), 963—973.

Dietrich, C.R., Newsam, G.N., 1993. A fast and exact method for multidimensional Gaussian stochastic simulations. Water Resources Research 29, 2861—2869.

Domenico, P.A., Schwartz, F.W., 1998. Physical and Chemical Hydrogeology. J. Wiley and sons.

Doughty, C., Karasaki, K., 2002. Flow and transport in hierarchically fractured rocks. Journal of Hydrology (263), 1—22.

Eames, I., Bush, J.W.M., 1999. Longitudinal dispersion by bodies fixed in a potential flow. Proceedings of Royal Society of London 455, 3665—3686.

Feehley, C.E., Zheng, C., Molz, F.J., 2000. A dual-domain mass transfer approach for modeling solute transport in heterogeneous aquifers: application to the Macrodispersion Experiment (MADE) site. Water Resources Research 36 (9), 2501—2515.

Fetter, C.W., 1999. Contaminant Hydrology, second ed. Prentice-Hall, Englewood Cliffs, New Jersey.

Fiori, A., Dagan, G., 2003. Time-dependent transport in heterogeneous formations of bimodal structure. 2. Results. Water Resources Research 39 (5). doi:10.1029/2002WR001398.

Fiori, A., Jankovic, I., Dagan, G., 2003a. Flow and transport in highly heterogeneous formations. 2. Semianalytical results for isotropic media. Water Resources Research 39 (9). doi:10.1029/2002WR001719.

Fiori, A., Jankovic, I., Dagan, G., 2003b. Flow and transport through two-dimensional isotropic media of binary conductivity distribution. Part 1: Numerical methodology and semi-analytical solutions. Stochastic Environmental Research and Risk Assessment 17, 370—383.

Fiori, A., Jankovic, I., Dagan, G., 2006. Modeling flow and transport in highly heterogeneous three-dimensional aquifers: ergodicity, Gaussianity, and anomalous behavior. 2. Approximate semi-analytical solutions. Water Resources Research 42. doi:10.1029/2005WR004752.

Fried, J.J., 1975. Groundwater Pollution. Elsevier.

Gelhar, L.W., 1993. Stochastic Subsurface Hydrology. Prentice-Hall, Englewood Cliffs, New Jersey.

Gelhar, L.W., Axness, C.L., 1983. Three-dimensional stochastic analysis of macrodispersion in aquifers. Water Resources Research 19 (1), 161—180.

Gelhar, L.W., Gutjahr, A.L., Naff, R.L., 1979. Stochastic analysis of macrodispersion in a stratified aquifer. Water Resources Research 15 (6), 1387—1397.

Gelhar, L.W., Welty, C., Rehfeldt, K.R., 1992. A critical review of data on field-scale dispersion in aquifers. Water Resources Research 28 (7), 1955—1974.

Gerke, H.H., van Genuchten, M.T., 1993. A dual-porosity model for simulating the preferential movement of water and solutes in structured porous media. Water Resources Research 29 (2), 305—319.

Ginn, T.R., 2001. Stochastic-convective transport with nonlinear reactions and mixing: finite streamtube ensemble formulation for multicomponent reaction systems with intra-streamtube dispersion. Journal of Contaminant Hydrology 47, 1—28.

Golfier, F., Quintard, M., Cherblanc, F., Zinn, B.A., Wood, B.D., 2007. Comparison of theory and experiment for solute transport in highly heterogeneous porous medium. Advances in Water Resources 30 (11), 2235—2261.

Gomez-Hernàndez, J.J., Sahuquillo, A., Capilla, J.E., 1997. Stochastic simulation of transmissivity fields conditional to both transmissivity and piezometric data. 1. Theory. Journal of Hydrology 203, 162—174.

Gomez-Hernàndez, J.J., Wen, X.-H., 1998. To be or not to be multi-Gaussian? A reflection on stochastic hydrogeology. Advances in Water Resources 21 (1), 47—61.

Greenkorn, R.A., 1983. Flow Phenomena in Porous Media. Marcel Dekker.

Griffioen, J., 1998. Suitability of the first-order mass transfer concept for describing cyclic diffusive mass transfer in stagnant zones. Journal of Contaminant Hydrology 34, 155—165.

Griffioen, J.W., Barry, D.A., Parlange, J.-Y., 1998. Interpretation of two-region model parameter. Water Resources Research 34 (3), 373—384.

Guswa, A.J., Freyberg, D.L., 2000. Slow advection and diffusion through low permeability inclusions. Journal of Contaminant Hydrology 46 (3—4), 205—232.

Haggerty, R., Gorelick, S.M., 1995. Multiple-rate mass transfer for modeling diffusion and surface reactions in media with pore-scale heterogeneity. Water Resources Research 31 (10), 2383—2400.

Haggerty, R., McKenna, S., Meigs, L.C., 2000. On the late-time behavior of tracer test breakthrough curves. Water Resources Research 36 (12), 3467—3479.

Haggerty, R., Harvey, C.F., Freiherr von Schwerin, C., Meigs, L.C., 2004. What controls the apparent timescale of solute mass transfer in aquifer and soils? A comparison of experimental results. Water Resources Research 40. doi:10.1029/2002WR001716.

Hantush, M.M., Marino, M.A., 1998a. Interlayer diffusive transfer and transport of contaminants in stratified formations I. Theory. Journal of Hydrologic Engineering 3 (4), 232—240.

Hantush, M.M., Marino, M.A., 1998b. Interlayer diffusive transfer and transport of contaminants in stratified formations IIAnalytical solutions. Journal of Hydrologic Engineering 3 (4), 241—246.

Harbaugh, A.W., Banta, E.R. Hill, M.C., McDonald, M.G., 2000. Modflow-2000, the U.S. Geological Survey modular ground-water model. User guide to modularization concepts and the ground-water flow process. Technical Report 00-92, USGS.

Harvey, C.F., Gorelick, S.M., 1995. Mapping hydraulic conductivity: sequential conditioning with measurement of solute arrival time, hydraulic head, and local conductivity. Water Resources Research 31 (7), 1615—1626.

Harvey, C., Gorelick, S.M., 2000. Rate-limited mass transfer or macrodispersion: which dominates plume evolution at the Macrodispersion Experiment (MADE) site? Water Resources Research 36 (3), 637—650.

Hassan, A.E., Cushman, J.H., Delleur, J.W., 1997. Monte Carlo studies of flow and transport in fractal conductivity fields: comparison with stochastic perturbation theory. Water Resources Research 33 (11), 2519—2534.

Hassanizadeh, S.M., 1996. On the transient non-Fickian dispersion theory. Transport in Porous Media 23, 107—124.

Hauns, M., Jeannin, P.-Y., Atteia, O., 2001. Dispersion, retardation and scale effect in tracer breakthrough curves in karst conduits. Journal of Hydrology 241, 277—293.

Hendricks Franssen, H.-J., Gomez-Hernàndez, J., Sahuquillo, A., 2003. Coupled inverse modeling of groundwater flow and mass transport and the worth of concentration data. Journal of Hydrology 281, 281—295.

Hess, K.M., Wolf, S.H., Celia, M.A., 1992. Large-scale natural gradient tracer test in sand and gravel, Cape Cod, Massachussetts. 3. Hydraulic conductivity variability and calculated macrodispersivities. Water Resources Research 28 (8), 2011—2027.

Huang, K., van Genuchten, M.T., Zhang, R., 1996. Exact solutions for one-dimensional transport with asymptotic scale-dependent dispersion. Applied Mathematics Modeling 20, 298—308.

Huang, H., Hu, B.X., 2000. Nonlocal nonreactive transport in heterogeneous porous media with interregional mass diffusion. Water Resources Research 36 (7), 1665—1675.

Huang, H., Hassan, A.E., Hu, B.X., 2003. Monte Carlo study of conservative transport in heterogeneous dual-porosity media. Journal of Hydrology 275, 229–241.

Hubbard, S.S., Rubin, Y., 2000. Hydrogeological parameter estimation using geophysical data: a review of selected techniques. Journal of Contaminant Hydrology 45, 3–34.

Hubbard, S.S., Chen, J., Peterson, J., Majer, E., Williams, K., Swift, D., et al., 2001. Hydrogeological characterization of the South Oyster bacterial transport site using geophysical data. Water Resources Research 37 (10), 2431–2456.

Hunt, B., 1998. Contaminant sources solutions with scale-dependent dispersivities. Journal of Hydrologic Engineering 3 (4), 268–275.

Hunt, B., 2002. Scale-dependent dispersion from a pit. Journal of Hydrologic Engineering 7 (2), 168–174.

Jaekel, U., Georgescu, A., Vereecken, H., 1996. Asymptotic analysis of nonlinear equilibrium solute transport in porous media. Water Resources Research 32 (10), 3093–3098.

Jankovic, I., Fiori, A., Dagan, G., 2003a. Flow and transport in highly heterogeneous formations. 3. Numerical simulations and comparison with theoretical results. Water Resources Research 39 (9). doi:10.1029/2002WR001721.

Jankovic, I., Fiori, A., Dagan, G., 2003b. Flow and transport through two-dimensional isotrophic media of binary conductivity distribution. Part 2: Numerical simulations and comparison with theoretical results. Stochastic Environmental Research and Risk Assessment 17, 384–393.

Jankovic, I., Fiori, A., Dagan, G., 2006. Modeling flow and transport in highly heterogeneous three-dimensional aquifers: ergodicity, Gaussianity, and anomalous behavior. 1. Conceptual issues and numerical simulations. Water Resources Research 42. doi:10.1029/2005WR004734.

Jarvis, N.J., Jansson, P.-E., Dik, P.E., Messing, I., 1991. Modeling water and solute transport in macroporous soil. I. Model description and sensitivity analysis. European Journal of Soil Science 42 (1), 59–70.

Javaux, M., Vanclooster, M., 2003. Scale- and rate-dependent solute transport within an unsaturated sandy monolith. Soil Science Society of America Journal 67 (5), 1334–1343.

Kemblowski, M.W., Wen, J.-C., 1993. Contaminant spreading in stratified soils with fractal permeability distribution. Water Resources Research 29 (2), 419–425.

Kemna, A., Vanderborght, J., Kulessa, B., Vereecken, H., 2002. Imaging and characterisation of subsurface solute transport using electrical resistivity tomography and equivalent transport models. Journal of Hydrology (267), 125–146.

Kilbas, A.A., Srivastava, H.M., Trujillo, J.J., 2006. Theory and Applications of Fractional Differential Equations. Elsevier, Amsterdam.

Klotz, D., Seiler, K.-P., Moser, H., Neumaier, F., 1980. Dispersivity and velocity relationship from laboratory and field experiments. Journal of Hydrology 45, 169–184.

Kohlbecker, M.V., Wheatcraft, S.W., Meerschaert, M.M., 2006. Heavy-tailed log hydraulic conductivity distributions imply heavy-tailed log velocity distributions. Water Resources Research 42. doi:10.1029/2004WR003815.

Kolwankar, K.M., Gangal, A.D., 1996. Fractional differentiability of nowhere differentiable functions and dimensions. Chaos 6, 505–524.

Labolle, E.M., 2000. RWHet: Random Walk Particle Model for Simulating Transport in Heterogeneous Permeable Media Version 2.0. University of California, Davis.

Lallemand-Barrès, A., Peaudecerf, P., 1978. Recherche des relations entre la valeur de la dispersivité macroscopique d'un milieu aquifère, ses autres caractéristiques et les conditions de mesure. Etude bibliographique. Bulletin du BRGM 2e série — Section III (4), 277–284.

Lambot, S., Slob, E.C., van den Bosch, I., Stockbroeckx, B., Scheers, B., Vanclooster, M., 2004. Estimating soil electric properties from monostatic ground-penetrating radar signal inversion in the frequency domain. Water Resources Research 40. doi:10.1029/2003WR002095.

Lessoff, S.C., Dagan, G., 2001. Solute transport in heterogeneous formations of bimodal conductivity distribution 2. Applications. Water Resources Research 37 (3), 473–480.

Lévy, P., 1937. Théorie de l'Addition des Variables Aléatoires. Gauthier-Villars, Paris.

Liu, H.H., Molz, F.J., 1997. Multifractal analyses of hydraulic conductivity distributions. Water Resources Research 33 (11), 2483–2488.

Logan, J.D., 1996. Solute transport in porous media with scale-dependent dispersion and periodic boundary conditions. Journal of Hydrology 184, 261–276.

Lu, S., Molz, F.J., Fogg, G.E., Castle, J.W., 2002. Combining stochastic facies and fractal models to represent natural heterogeneity. Hydrogeology Journal (10), 475–482.

Luo, J., Cirpka, O.A., Fienen, M.N., Wu, W.-M., Mehlhorn, T.L., Carley, J., Jardine, P.M., Criddle, C.S., Kitanidis, P.K., 2006. A parametric transfer function methodology for analyzing reactive transport in nonuniform flow. Journal of Contaminant Hydrology 83, 27–41.

Maas, C., 1999. A hyperbolic dispersion equation to model the bounds of a contaminated groundwater body. Journal of Hydrology 226, 234–241.

Mandelbrot, B., 1983. The Fractal Geometry of Nature. W.H. Freeman, New York.

Margolin, G., Berkowitz, B., 2000. Application of continuous time random walk to transport in porous media. Journal of Physical Chemistry B 104, 3942–3947.

Margolin, G., Berkowitz, B., 2002. Spatial behavior of anomalous transport. Physical Review E, 65.

Margolin, G., Berkowitz, B., 2004. Continuous time random walk revisited: first passage time and spatial distributions. Physica A 334, 46–66.

Maxwell, R.M., Chow, F.K., Kollet, S.J., 2007. The groundwater-land-surface-atmosphere connection: soil moisture effects on the atmospheric boundary layer in fully-coupled simulations. Advances in Water Resources 30, 2447–2466.

Meerschaert, M.M., Benson, D.A., Baeumer, B., 1999. Multidimensional advection and fractional dispersion. Physical Review E 59 (5), 5026–5028.

Meerschaert, M.M., Benson, D.A., Baeumer, B., 2001. Operator Lévy motion and multiscaling anomalous diffusion. Physical Review E 63, 1112–1117.

Meerschaert, M.M., Benson, D.A., Scheffler, H.-P., Baeumer, B., 2002. Stochastic solution of space–time fractional diffusion equations. Physical Review E 65 (4), 102–105.

Metzler, R., Klafter, J., 2000. The random walk's guide to anomalous diffusion: a fractional dynamics approach. Physics Reports 339, 1–77.

Miller, K.S., Ross, B., 1993. An Introduction to the Fractional Calculus and Fractional Differential Equations. John Wiley and Sons.

Molz, F.J., Boman, G.K., 1995. Further evidence of fractal structure in hydraulic conductivity distributions. Geophysical Research Letter 22 (18), 2545–2548.

Molz, F.J., Liu, H.H., Szulga, J., 1997. Fractional Brownian motion and fractional Gaussian noise in subsurface hydrology: a review, presentation of fundamental properties, and extensions. Water Resources Research 33 (10), 2273–2286.

Molz, F.J., Rajaram, H., Lu, S., 2004. Stochastic fractal-based models of heterogeneity in subsurface hydrology: origin, applications, limitations, and future research questions. Review of Geophysics 42, doi: 2003RG000,126.

Monnig, N.D., Benson, D.A., Meerschaert, M.M., 2008. Ensemble solute transport in two-dimensional operator-scaling random fields. Water Resources Research 44, W02434. doi:10.1029/2007WR005998.

Moyne, C., 1996. Two-equation model for a diffusive process in porous media using the volume-averaging method with an unsteady state closure. Advances in Water Resources 20 (2-3), 63–76.

Muller, J., 1996. Characterization of pore space in chalk by multifractal analysis. Journal of Hydrology 187, 215–222.

Neuman, S.P., 1993. Eulerian–Lagrangian theory of transport in space-time nonstationary velocity field: exact nonlocal formalism by conditional moments and weak approximation. Water Resources Research 29 (3), 633–645.

Neuman, S.P., 1995. On advective transport in fractal permeability and velocity fields. Water Resources Research 31 (6), 1455–1460.

Neuman, S.P., Winter, C.L., Newman, C.M., 1987. Stochastic theory of field-scale Fickian dispersion in anisotropic porous media. Water Resources Research 23 (3), 453–466.

Neuman, S.P., Orr, S., 1993. Prediction of steady-state flow in nonuniform geologic media by conditional moments — exact nonlocal formalism, effective conductivities, and weak approximation. Water Resources Research 29 (2), 341–364.

Nkedi-Kizza, P., Biggar, J.W., Selim, H.M., van Genuchten, M.T., Wierenga, P.J., Davidson, J.M., Nielsen, D.R., 1984. On the equivalence of two conceptual models for describing ion exchange during transport through an aggregated oxisol. Water Resources Research 20 (8), 1123–1130.

Pachepsky, Y., Timlin, D., 1998. Water transport in soils as in fractal media. Journal of Hydrology 204, 98–107.

Painter, S., 1996. Evidence for non-Gaussian scaling behavior in heterogeneous sedimentary formations. Water Resources Research 32 (5), 1183–1196.

Painter, S., Paterson, L., 1994. Fractional Lévy motion as a model for spatial variability in sedimentary rocks. Geophysical Research Letter 21 (25), 2857–2860.

Panfilov, M., 2000. Models of Flow Through Highly Heterogeneous Porous Media. Kluwer, Dordrecht.

Pang, L., Hunt, B., 2001. Solutions and verification of a scale-dependent dispersion model. Journal of Contaminant Hydrology (53), 21–39.

Parker, J.C., Valocchi, A.J., 1986. Constraints on the validity of equilibrium and first-order kinetic models in structured soils. Water Resources Research 22 (3), 399–407.

Peters, G.P., Smith, D.W., 2000. Spatially and temporally varying dispersivity. In: GeoEng 2000 Conference Proceedings.

Pickens, J.F., Grisak, G.E., 1981. Modeling of scale-dependent dispersion in hydrogeologic systems. Water Resources Research 17 (6), 1701–1711.

Quintard, M., Cherblanc, F., Whitaker, S., 2001. Dispersion in heterogeneous porous media: one equation equilibrium model. Transport in Porous Media 44, 181–203.

Rajaram, H., Gelhar, L.W., 1993. Plume-scale dependent dispersion in heterogeneous aquifers 2. Eulerian analysis and three-dimensional aquifers. Water Resources Research 29 (9), 3261–3276.

Rajaram, H., Gelhar, L.W., 1995. Plume-scale dependent dispersion in aquifers with a wide range of scales of heterogeneity. Water Resources Research 31 (10), 2469–2482.

Rao, P.S.C., Rolston, D.E., Jessup, R.E., Davidson, J.M., 1980. Solute transport in aggregated porous media: theoretical and experimental evaluation. Soil Science Society of America Journal 44, 1139–1146.

Reeves, D.M., Benson, D.A., Meerschaert, M.M., Scheffler, H.-P., 2008. Transport of conservative solutes in simulated fracture networks: 2 Ensemble solute transport and the correspondence to operator-stable limit distributions. Water Resources Research 44, W05410. doi:10.1029/2008WR006858.

Rubin, Y., 1995. Flow and transport in bimodal heterogeneous formations. Water Resources Research 31 (10), 2461–2468.

Rubin, Y., 2003. Applied Stochastic Hydrogeology. Oxford University Press, New York.

Rubin, Y., Dagan, G., 1988. Stochastic analysis of the effects of boundaries on spatial variability in groundwater flows: 1 Constant head boundary. Water Resources Research 24 (10), 1689–1697.

Rubin, Y., Dagan, G., 1989. Stochastic analysis of the effects of boundaries on spatial variability in groundwater flows: 2 Impervious boundary. Water Resources Research 25 (4), 707–712.

Rubin, Y., Sun, A., Maxwell, R., Bellin, A., 1999. The concept of block-effective macrodispersivity and a unified approach for grid-scale- and plume-scale-dependent transport. Journal of Fluid Mechanics 395, 161–180.

Salandin, P., Fiorotto, V., 1998. Solute transport in highly heterogeneous aquifers. Water Resources Research 34 (5), 949–961.

Samko, S.G., Kilbas, A.A., Marichev, O.I., 1993. Fractional Integrals and Derivatives: Theory and Applications. Gordon and Breach Science Publishers.

Sauty, J., 1978. Mise au point et utilisation d'abaques pour l'interprétation des expériences de tracedilcages dans les nappes d'eau souterraine. Bulletin du BRGM — 2e série-section III (4), 285–291.

Sauty, J., 1980. An analysis of hydrodispersive transfer in aquifers. Water Resources Research 16 (1), 145–158.

Scheidegger, A.E., 1958. Typical solutions of the differential equations of statistical theories of flow through porous media. Transactions, American Geophysical Union 39 (5), 929–932.

Scheidegger, A.E., 1960. The Physics of Flow through Porous Media. Mac-Millan Company.

Schumer, R., Benson, D.A., Meerschaert, M.M., Wheatcraft, S.W., 2001. Eulerian derivation of the fractional advection–dispersion equation. Journal of Contaminant Hydrology (48), 69–88.

Schumer, R., Benson, D.A., Meerschaert, M.M., Baeumer, B., 2003a. Fractal mobile/immobile solute transport. Water Resources Research 39 (10). doi:10.1029/2003WR002141.

Schumer, R., Benson, D.A., Meerschaert, M.M., Baeumer, B., 2003b. Multiscaling fractional advection–dispersion equations and their solutions. Water Resources Research 39 (1).

Silliman, S.E., Simpson, E.S., 1987. Laboratory evidence of the scale effect in dispersion of solutes in porous media. Water Resources Research 23 (8), 1667–1673.

Simmons, C.S., 1982. A stochastic-convective transport representation of dispersion in one-dimensional porous media systems. Water Resources Research 18 (4), 1193–1214.

Simmons, C.S., Ginn, T.R., Simpson, E.S., 1995. Stochastic-convective transport with nonlinear reaction: mathematical framework. Water Resources Research 31 (11), 2675–2688.

Simunek, J., Jarvis, N.J., van Genuchten, M.T., Gardenas, A., 2003. Review and comparison of models for describing non-equilibrium and preferential flow and transport in the vadose zone. Journal of Hydrology 272, 14–35.

Sivakumar, B., Harter, T., Zhang, H., 2005. A fractal investigation of solute travel time in a heterogeneous aquifer: transition probability/Markov chain representation. Ecological Modeling 182, 355–370.

Slater, L., Binley, A.M., Daily, W., Johnson, R., 2000. Cross-hole electrical imaging of a controlled saline tracer injection. Journal of Applied Geophysics 44, 85–102.

Sposito, G., White, R.E., Darrah, P.R., Jury, W.A., 1986. A transfer-function model of solute transport through soil. 3. The convection–dispersion equation. Water Resources Research 22 (2), 255–262.

Stauffer, F., Rauber, M., 1998. Stochastic macrodispersion model for gravel aquifers. Journal of Hydraulic Research 36 (6), 885–896.

Strack, O.D.L., 1992. A mathematical model for dispersion with a moving front in groundwater. Water Resources Research 28 (11), 2973–2980.

Sudicky, E.A., 1986. A natural gradient experiment on solute transport in a sand aquifer: spatial variability of hydraulic conductivity and its role in the dispersion process. Water Resources Research 22 (13), 2069–2082.

Taylor, S.R., Howard, K.W.F., 1987. A field study of scale-dependent dispersion in a sandy aquifer. Journal of Hydrology 90, 11–17.

Teles, V., Delay, F., de Marsily, G., 2004. Comparison of genesis and geostatistical methods for characterizing the heterogeneity of alluvial media: groundwater flow and transport simulations. Journal of Hydrology 294, 103–121.

Tennekoon, L., Boufadel, M.C., Lavallee, D., Weaver, J., 2003. Multifractal anisotropic scaling of the hydraulic conductivity. Water Resources Research 39 (7). doi:10.1029/2002WR001645.

Tompson, A.F.B., 1988. On a new functional form for the dispersive flux in porous media. Water Resources Research 24 (11), 1939–1947.

Tompson, A.F.B., Gray, W.G., 1986. A 2nd-order approach for the modeling of dispersive transport in porous media 1. Theoretical development. Water Resources Research 22 (5), 591–599.

Tompson, A.F.B., Gelhar, L.W., 1990. Numerical simulation of solute transport in three-dimensional, randomly heterogeneous porous media. Water Resources Research 26 (10), 2541–2562.

Toride, N., Leij, F.J., van Genuchten, M.T., 1995. The CXTFit code for estimating transport parameters from laboratory or field tracer experiments. Technical Report, Research Report 137, U.S. Salinity Laboratory, Agricultural Research Service, U.S. Department of Agriculture, Riverside, California.

Trefry, M.G., Ruan, F.P., McLaughlin, D., 2003. Numerical simulations of preasymptotic transport in heterogeneous porous media: departures from the Gaussian limit. Water Resources Research 39 (3). doi:10.1029/2001WR001101.

Valocchi, A.J., 1985. Validity of the local equilibrium assumption for modeling sorbing solute transport through homogeneous soils. Water Resources Research 21 (6), 808–820.

van Genuchten, M.T., Wierenga, P.J., 1976. Mass transfer studies in sorbing porous media. I. Analytical solutions. Soil Science Society of America Journal 40 (4), 473–480.

van Genuchten, M.T., Tang, D.H., Guennelon, R., 1984. Some exact solutions for solute transport through soils containing large cylindrical macropores. Water Resources Research 20 (3), 335–346.

van Genuchten, M.T., Wagenet, R.J., 1989. Two-site/two-region models for pesticide transport and degradation: theoretical development and analytical solutions. Soil Science Society of America Journal 53 (5), 1303–1310.

Vogel, H.-J., Roth, K., 2003. Moving through scales of flow and transport in soils. Journal of Hydrology 272, 95–106.

Wang, P.P., Zheng, C., Gorelick, S.M., 2005. A general approach to advective–dispersive transport with multirate mass transfer. Advances in Water Resources 28, 33–42.

Weissmann, G.S., Carle, S.F., Fogg, G.E., 1999. Three-dimensional hydrofacies modeling based on soil surveys and transition probability geostatistics. Water Resources Research 35 (6), 1761–1770.

Wen, X.-H., Gomez-Hernàndez, J.J., 1996. Upscaling hydraulic conductivities in heterogeneous media: an overview. Journal of Hydrology 183, 9–23.

Wheatcraft, S.W., Tyler, S.W., 1988. An explanation of scale-dependent dispersivity using concepts of fractal geometry. Water Resources Research 24 (4), 566–578.

Whitaker, S., 1999. The Method of Volume Averaging. Kluwer, Dordrecht.

Yates, S.R., 1990. An analytical solution for one-dimensional transport in heterogeneous porous media. Water Resources Research 26 (10), 2331–2338.

Zappa, G., Bersezio, R., Felletti, F., Guidici, M., 2006. Modeling heterogeneity of gravel-sand, braided stream, alluvial aquifers at the facies scale. Journal of Hydrology 325, 134–153.

Zhan, H., Wheatcraft, S.W., 1996. Macrodispersivity tensor for nonreactive solute transport in isotropic and anisotropic fractal porous media: analytical solutions. Water Resources Research 32 (12), 3461–3474.

Zhang, Y., Benson, D.A., Baeumer, B., 2007a. Predicting the tails of breakthrough curves in regional-scale alluvial systems. Ground Water 45 (4), 473–484.

Zhang, Y., Benson, D.A., Meerschaert, M.M., Labolle, E.M., 2007b. Space-fractional advection–dispersion equations with variable parameters: diverse formulas, numerical solutions, and application to the Macrodispersion Experiment site data. Water Resources Research 43. doi:10.1029/2006WR004912.

Zhang, Y., Benson, D.A., LaBolle, E.M., Reeves, D.M., 2008. Fractional RWHet: An enhanced solver for solute transport with both spatiotemporal memory and conditioning on local aquifer properties. In: Proceedings of MODFLOW and MORE 2008: Ground Water and Public Policy, May 19–21, Golden, CO, pp. 62–66.

Zhou, L., Selim, H.M., 2002. A conceptual fractal model for describing time-dependent dispersivity. Soil Science 167 (3), 173–183.

Zhou, L., Selim, H.M., 2003. Scale-dependent dispersion in soils: an overview. Advances in Agronomy 80, 223–263.

Zinn, B., Meigs, L.C., Harvey, C.F., Haggerty, R., Peplinski, W.J., Freiherr von Schwerin, C., 2004. Experimental visualization of solute transport and mass transfer processes in two-dimensional conductivity fields with connected regions of high conductivity. Environmental Science and Technology 38, 3916–3926.

Zou, S., Xia, J., Koussis, A.D., 1996. Analytical solutions to non-Fickian subsurface dispersion in uniform groundwater flow. Journal of Hydrology (179), 237–258.